Arsenic Adsorption Characteristics of Magnetite Nanoparticles

by

Preetom Kishore Roy

MASTER OF SCIENCE IN CIVIL ENGINEERING (ENVIRONMENTAL)

Department of Civil Engineering

BANGLADESH UNIVERSITY OF ENGINEERING AND TECHNOLOGY

2009

বাংলাদেশ প্রকৌশল বিশ্ববিদ্যালয়
নং 107242
তাং 23.06.09
লাইব্রেরী, ঢাকা

#107242#

Arsenic Adsorption Characteristics of Magnetite Nanoparticles

by

Preetom Kishore Roy

A thesis submitted to the Department of Civil Engineering of Bangladesh University of Engineering and Technology, Dhaka, in partial fulfilment of the requirements for the degree of

MASTER OF SCIENCE IN CIVIL ENGINEERING (ENVIRONMENTAL)

2009

The thesis titled **"Arsenic Adsorption Characteristics of Magnetite Nanoparticles"** submitted by Preetom Kishore Roy, Student No. 100604128(P), and Session: October 2006 has been accepted as satisfactory in partial fulfilment of the requirement for the degree of M.Sc. Engineering (Civil and Environmental) on 25th April, 2009.

BOARD OF EXAMINERS

Dr. M. Ashraf Ali Professor Department of Civil Engineering, BUET, Dhaka	**Chairman** (Supervisor)
Dr. Muhammad Zakaria Professor and Head Department of Civil Engineering, BUET, Dhaka	**Member** (Ex-officio)
Dr. Md. Delwar Hossain Professor Department of Civil Engineering, BUET, Dhaka	**Member**
Dr. Ganesh Chandra Saha Professor Department of Civil Engineering, DUET Gazipur 1700, Bangladesh	**Member** (External)

DECLARATION

I, hereby declare that the research work reported in this thesis has been performed by me and this work or any part of it has not been submitted elsewhere for the award of any degree or diploma.

25 April, 2009

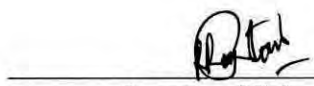

Preetom Kishore Roy

Dedicated

To

My Family & My Friends

ACKNOWLEDGEMENT

First of all I want to pay my heartiest gratitude and profound indebtedness to my thesis supervisor, Dr. M. Ashraf Ali, for providing me continuous support and guideline to perform this research work and to prepare this thesis. His contribution to me can only be acknowledged but never be compensated. His consistent inspiration along with valuable advice throughout the study was a great help in completion of this research work.

I would like to express my deepest gratitude to the Department of Civil Engineering, BUET, The Head of the Department of Civil Engineering and all the members of BPGS committee to give me such a great opportunity of doing my M.Sc. and this contemporary research work on environmental nanotechnology. I would like to furnish my sincere gratitude to Dr. A.B.M. Badruzzaman for providing assistance to this study through MIT-BUET joint research project and also for providing effective guidance and support throughout the course of this thesis work.

I would like to convey my heartiest thanks especially to Dr. Navid Bin Saleh (currently an Assistant Professor at University of South Carolina, USA), who performed the characterization tests (DLS analysis, BET analysis) of the magnetite nanoparticles. Dr. Navid Bin Saleh provided me with his valuable time and effort from his busy research schedules to perform the DLS and BET experiments in the laboratory of Yale University, where he worked as a Post-doctoral Research Associate. Also I would like to thank Dr. Manjura Hoque, Atomic Energy Commission, Dhaka, Bangladesh for performing the XRD analysis of the magnetite nanoparticles.

Furthermore, I want to thank Mr. Ehsan and Mr. Mithu of Environmental Engineering Laboratory, BUET, for frequent support in my laboratory work through out the entire thesis work.

I would like to convey my gratefulness and thanks to all my family members, friends and colleagues.

At last I want to thank all the members of the defence board and respected supervisor Dr. M. Ashraf Ali once again for giving me such an opportunity, which has obviously enhanced my knowledge and skills to a great extent in the arena of environmental engineering.

Preetom Kishore Roy

TABLE OF CONTENTS

List of Figures

List of Tables

Acronyms

AAS	Atomic Absorption Spectrophotometer
BAMWSP	Bangladesh Arsenic Mitigation and Water Supply Program
BET	Brunauer-Emmett-Teller
BGS	British Geological Survey
CHES	2-(Cyclohexylamino) Ethane-Sulfonic Acid
DLS	Dynamic Light Scattering
DPHE	Department Of Public Health Engineering
HEPES	2-[4-(2-Hydroxyethyl)-1-Piperazine] Ethanesulfonic Acid
HNP	Hematite Nanoparticle
MES	2-Morpholinoethanesulfonic Acid Monohydrate
MNP	Magnetite Nanoparticle
HEPES	2-[4-(2-Hydroxyethyl)-1-Piperazine] Ethanesulfonic Acid
MES	2-Morpholinoethanesulfonic Acid Monohydrate
MNP	Magnetite Nanoparticle
SFCA	Surfactant Free Cellulose Acetate
SSA	Specific Surface Area
TEM	Transmission Electron Microscope
USEPA	United States Environmental Protection Agency
WHO	World Health Organization
XRD	X-Ray Diffraction

বাংলাদেশ প্রকৌশল বিশ্ববিদ্যালয়
নং 107242
তাং 23.06.09
লাইব্রেরী, ঢাকা

Chapter 1

INTRODUCTION

1.1 General

Access to safe drinking water in sufficient quantity is a basic requirement for human life. Safe drinking water is rarely found in the nature. In Bangladesh, there are two major sources of water – surface water and groundwater. The surface water often contains pathogenic microorganisms responsible for water borne diseases. Pathogenic contamination of water is the primary reason behind the prevalence of diarrheal diseases in Bangladesh, particularly in rural areas. The water supply in Bangladesh, particularly in rural water supply, is almost entirely based on groundwater which is extracted primarily by shallow tube-well. Groundwater extracted from shallow aquifers using hand-tube-wells is the primary source of drinking and cooking water for most of its population.

In recent years widespread arsenic contamination of groundwater has become a major concern for the hand tube-well based drinking water supply, particularly in the rural areas. Awareness about the presence of arsenic has been growing since late 1993 when arsenic was first detected in the district of Chapai Nawabganj bordering the West-Bengal district of India. Out of 64 administrative districts of Bangladesh, arsenic contamination has so far been reported in 61 districts and an estimated 40 million people are at risk of arsenic toxicity. In Bangladesh presence of dissolved arsenic in shallow groundwater above acceptable level is a major public health concern.

Bangladesh Arsenic Mitigation and Water Supply Program (BAMWSP) has compiled field-kit measurements of the arsenic content of groundwater for nearly five million wells (BAMWSP, 2005) across the most affected half of the country and provided the most extensive and detailed representation of the spatial distribution of arsenic in

groundwater of Bangladesh (Fig.1.1). A set of 270 of 490 Upazilas where a blanket survey of million tube-wells, were coordinated under BAMWSP and found that Bangladesh has been affected with significantly high concentrations of arsenic, with the greatest contamination in the south and south-east region of the country and least in the north-west and the uplifted areas in north central region which confirmed the survey work done by British Geological Survey (BGS/ DPHE, 2001).

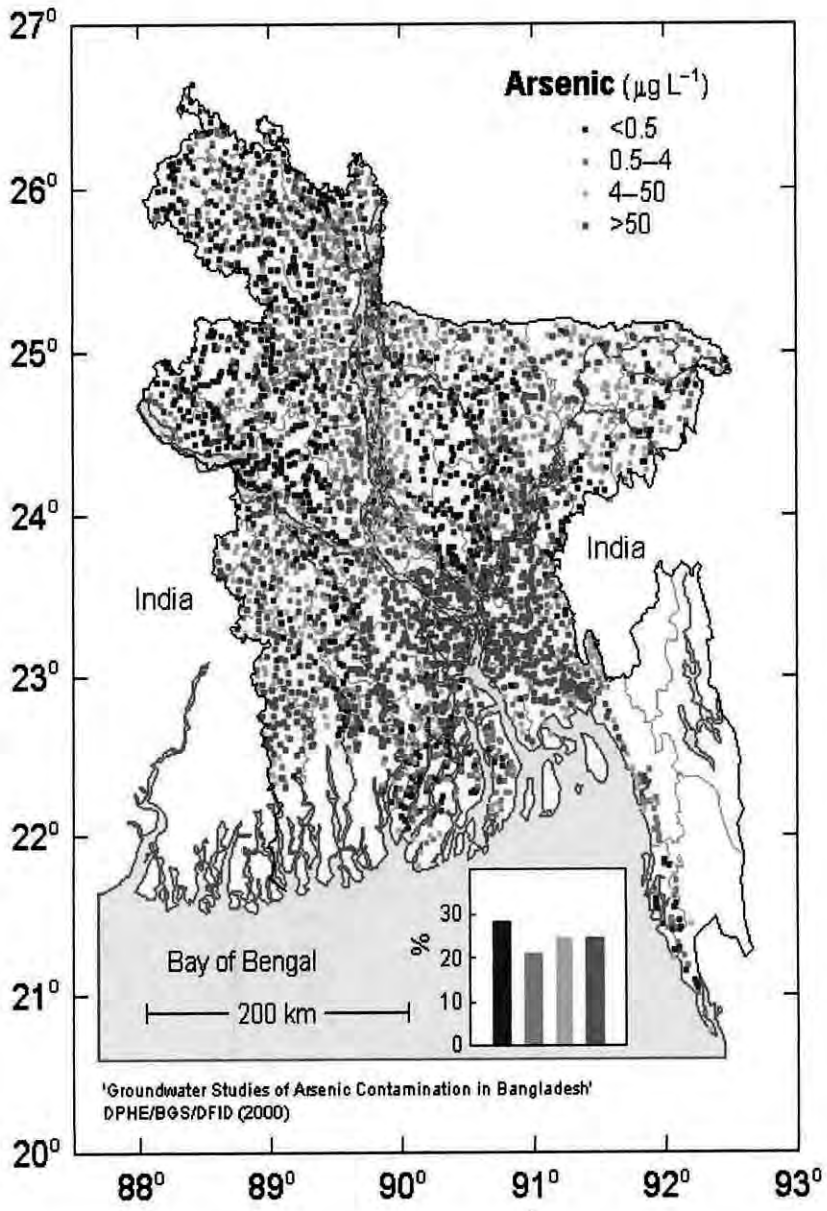

Figure 1.1. arsenic concentration in Bangladesh based on the nationwide survey carried out by BGS/DPHE, 2001.

Arsenic toxicity has no known effective medicine for treatment, but drinking of arsenic free water can help the arsenic affected people to get rid of the symptoms of arsenic toxicity. There is an urgent need to ensure supply of arsenic free drinking water to the millions of arsenic affected people in Bangladesh. The options that are commonly suggested as possible alternatives to arsenic affected groundwater include: (1) Arsenic free deep tube-well water; (2) Surface water, (3) Rainwater harvesting, and (4) Treatment of groundwater for arsenic removal. While arsenic-free deep aquifers have been identified in some places, this option appears to be too expensive for large scale use in rural areas. The principal problem with surface water is bacteriological contamination. In addition availability of surface water is not uniform throughout the year. Rainwater harvesting can be a probable alternative. But seasonal variation in rainfall pattern, proper storage of rainwater and public acceptance are some of the issues that need to be adequately addressed. Groundwater treated for arsenic removal is another very promising option to provide arsenic-free water to the rural population. Since people are already accustomed to using groundwater and millions of tube-wells are already there in the rural areas, this option can make use of this available infrastructure. It should be noted that only water used for drinking and cooking purposes need to be treated; so volume of water that need to be treated would not be very high.

Inorganic arsenic occurs in natural water primarily as As(V), arsenate and As(III), arsenite. In oxygen-rich waters, As(V) will be the predominant oxidation state with $H_2AsO_4^-$ and $HAsO_4^{2-}$ being the principal species. Under more reducing conditions, e.g., in groundwater, As(III) predominates, with H_3AsO_3 being the dominant species. A wide range of methods is available for arsenic removal from groundwater, each having its own advantages and disadvantages. These methods include anion exchange resins, granular iron-oxide based media, activated alumina, granular zirconia and titania, and iron/alum flocculation processes (Driehaus *et al.*, 1998; Berdal *et al.*, 2000; Rubel, 2003(a); Badruzzaman and Westerhoff, 2005). Polymeric anion exchange resins have a low selectivity for arsenate and certain anions such as sulfate competes with arsenate for available anion exchange sites resulting in a short operational life. Many of the granular iron oxide-based, porous media have a very high affinity for arsenate and a negligible affinity for other common anions, such as

sulfate, bicarbonate, and chloride (Meng *et al.*, 2000), which means that they have high operational lives. However, a major drawback, which is causing operational problems, is the low structural stability of many of the granular media (North, 2005). In use, the media requires periodic backwashing to remove fines generated from the breakdown of the media granules. This backwash solution needs to be treated and safely disposed of, and additional capital equipment needs to be installed to facilitate the backwash process. These granular media cannot be regenerated due to their low physical strength. Coagulation using iron floc as a treatment method is highly effective at removing arsenic from water but generates large amounts of a ferric hydroxide floc, which will require safe disposal in a landfill. Capital equipment requirements are generally high, since a ferric hydroxide floc can be difficult to separate from solution effectively. Although chemical consumption is low, ferric floc systems require high levels of maintenance and are generally best suited to large municipal authorities where large volumes of water are being treated daily at a single location, making the system more cost effective. However, more detailed description about various conventional arsenic removal technologies are discussed in Chapter 2.

Numerous studies demonstrate that iron oxides have a high affinity for the adsorption of arsenite and arsenate. The surface properties of iron oxides are key factors in adsorption on iron oxides. However, the sorption behavior of arsenic is strongly influenced by solution pH values and presence of other competing ions (Dixit and Hering, 2003). Recently, iron nanomaterials have attracted considerable attention with regard to adsorption of trace contaminants due to their small particle size and large surface area. Nanomaterials exhibit different physical, chemical, and biological properties that may not be predictable from observations on larger-sized materials.

Nanoscale iron particles represent a new generation of environmental remediation technologies that could provide cost-effective solutions to some of the most challenging environmental cleanup problems. Nanoscale iron particles have large surface areas and high surface reactivity. Equally important, they provide enormous flexibility for *in situ* applications. Research has shown that nanoscale iron particles are very effective for the transformation and detoxification of a wide variety of common environmental contaminants, such as chlorinated organic solvents, organo

chlorine pesticides. Modified iron nanoparticles, such as catalyzed and supported nanoparticles have been synthesized to further enhance the speed and efficiency of remediation. Zhang (2003) provides assessment of the recent developments in both laboratory and pilot studies including: (1) synthesis of nanoscale iron particles (10–100 nm, >99.5% Fe) from common precursors such as Fe(II) and Fe(III); (2) reactivity of the nanoparticles towards contaminants in soil and water over extended periods of time (e.g., weeks); (3) field tests validating the injection of nanoparticles into aquifer, and (4) *in situ* reactions of the nanoparticles in the subsurface.

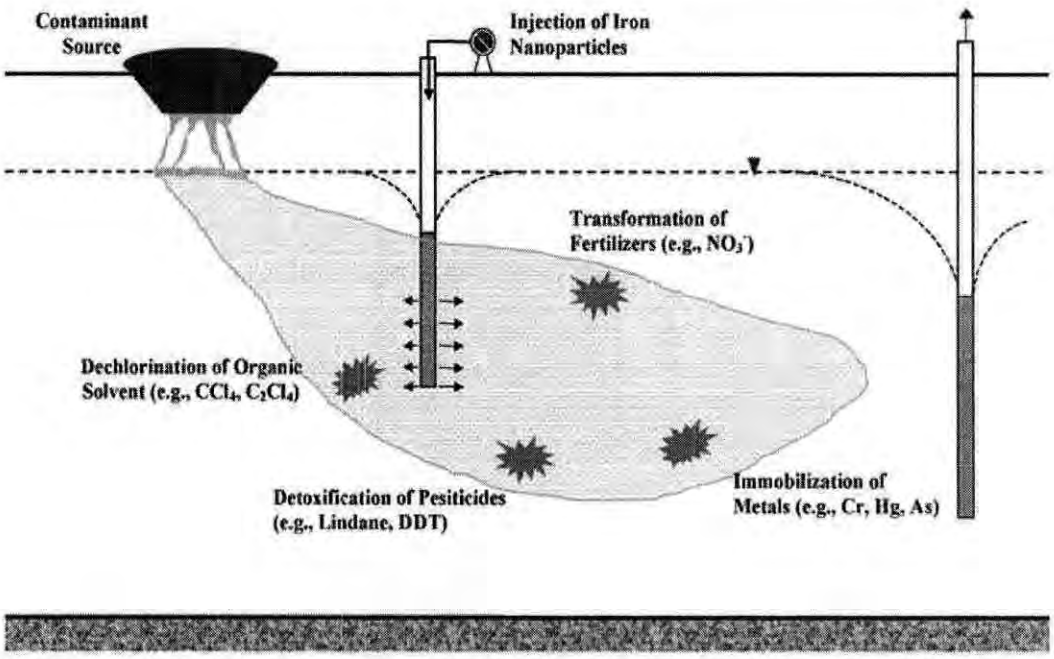

Figure 1.2. Nanoscale iron particles for *in situ* remediation (Zhang, 2003)

Recent research has suggested that as a remediation technique, nanoscale iron particles have several advantages: (1) effective for the transformation of a large variety of environmental contaminants, (2) inexpensive, and (3) nontoxic (Zhang, 2003).

ArsenX^{np} is a hybrid inorganic/organic sorbent (Sylvester *et al.*, 2005; Sylvester *et al.*, 2007) that has been developed for the removal of arsenic from drinking water and consists of hydrous iron oxide nanoparticles impregnated into 300–1200 μm durable polymeric beads. The nano size of the hydrous iron oxide particles results in a very

high surface area, and this, coupled with the high porosity of the polymer substrate, ensures that the rate of arsenic uptake is, at least initially, relatively rapid, and the arsenic removal capacity is high. The sorbent selectively sorbs both As(III) and As(V) species from solution with minimal competition from inert anions, such as sulfate, fluoride, bicarbonate, and chloride, that are present in drinking water at concentrations many orders of magnitude greater than arsenic (Sengupta and Cumbal, 2005). Dissolved silica, particularly at pH values above 7.5, and phosphate are the major species in drinking water that interfere with arsenic uptake by any iron-based adsorption media (Clifford, 2003).

In addition to nanoscale zero-valent iron (NZVI), which is a suitable material for both *in-situ* and *ex-situ* groundwater treatment, iron oxide nanoparticles are also suitably used for groundwater remediation.

Hydrated Iron Oxide is another effective adsorbent for removal of heavy metals such as arsenic. By appropriately dispersing HFO nanoparticles within a polymeric cation or anion exchanger, its amphoteric sorption capacity can be tailored to remove either metal cations or anionic ligands.

Because of their miniscale size, nanoparticles (e.g., magnetite, hematite nanoparticles) cannot be directly used in an arsenic removal system. Common options are either to use nanoparticle-water slurry or anchor nanoparticle in a solid matrix similar to generation of ArsenX^{np} (Sylvester *et al.*, 2005; Sylvester *et al.*, 2007), which them could be used for arsenic removal. For developing arsenic removal system, it is extremely important to characterize the nanomaterial itself (e.g., size, aggregation characterization) as well as their adsorption characterization.

Available literatures (Mayo *et al.*, 2007; Yean *et al.*, 2005) suggest that magnetite could potentially be used in the removal of arsenic from groundwater. So, in order to establish magnetite (Fe_3O_4) nanoparticles (MNPs) potential sorbents for arsenic removal in drinking water, detailed assessments of adsorption characteristics of arsenic on MNPs under different conditions are necessary.

1.2 Objectives of the Present Research

The overall objective of this study is to assess the adsorption characteristics of arsenic on magnetite nanoparticles. Specific objectives include:

1. Characterization (e.g., size, surface area, aggregation characterizations) of magnetite nanoparticles

2. Development of adsorption isotherms of arsenic on magnetic nanoparticles

3. Development of adsorption envelopes of arsenic on magnetite nanoparticles

4. Evaluation of adsorption kinetics of arsenic on magnetite nanoparticles

5. Assessment of the effect of pH and phosphate (competing anion) on adsorption of arsenic on magnetite nanoparticles.

The proposed research is expected to improve understanding of the effectiveness of magnetite nanoparticles as adsorbent for removal of arsenic from water. This research will also provide information on maximum arsenic adsorption capacities of magnetite at different pH values, and their comparison with other commonly used adsorbents. Results of this study would also enable an assessment of the potential of magnetite nanoparticles for development of arsenic removal systems.

1.3 Organization of the Thesis

Apart from this chapter, the remainder of the thesis has been divided into four chapters. Chapter-2 represents information (occurrence, sources, chemistry, and acute toxicity in humans) about arsenic in environment. Conventional arsenic removal technologies are also discussed in this chapter. The adsorption isotherms (Langmuir, Freundlich), and adsorption kinetics are also discussed in this chapter.

Chapter-3 represents the characterization of magnetite nanoparticles. This chapter discusses size and size distribution, specific surface area, structure and composition, and potential surface charge of magnetite nanoparticles determines through laboratory investigation in this study.

Chapter-4 presents the results of arsenic (both arsenate and arsenite) removal from water by adsorption onto magnetite nanoparticles. The effects of initial arsenic concentration, pH, time and competing anion (phosphate) are also discussed in this Chapter.

Finally, Chapter-5 represents major conclusions of the study and also provides recommendations for future study.

Chapter 2

LITERATURE REVIEW

2.1 Introduction

Numerous nanomaterials are in various stages of research and development, each possessing unique functionalities that are potentially applicable to the remediation of industrial wastewater, groundwater, surface water and drinking water. The main goal for most of this research is to develop low-cost and environmentally friendly materials for removal of heavy metals from water. For this purpose, the researchers are doing researches about nano sized particles to find out their various characteristics in order to make prominent use of such nanoparticles.

Magnetite (Fe_3O_4) nanoparticles are potential sorbents for arsenic removal in drinking water. Available literatures (Mayo *et al.*, 2007; Yean *et al.*, 2005) suggest that magnetite could potentially be used in the removal of arsenic from groundwater.

This Chapter represents occurrence, sources, chemistry, and acute toxicity in humans about arsenic in environment along with conventional arsenic removal technologies. The adsorption isotherms (Langmuir, BET, Freundlich), and adsorption kinetics for arsenic adsorption are also discussed here.

2.2 Occurrence of Arsenic

Arsenic ranks 20^{th} in abundance in the earth's crust. The average crustal abundance of arsenic is 1.5 mg/kg. The element is strongly chalocophile. Approximately 60% of natural arsenic minerals are arsenates, 20% sulphides and sulfosalts, and the remaining 20% are arsenides, arsenites, oxides, alloys and polymorphs of elemental arsenic. Arsenic concentrations of more than 10^5 mg/kg have been reported in

sulphide minerals and up to $7.6x10^4$ mg/kg in iron oxides (Smedley and Kinniburgh, 2002). However, concentrations are typically much lower. Arsenic is incorporated into primary rock-forming minerals only to a limited extent, for example, by the substitution of As^{3+} for Fe^{3+} or Al^{3+}. Therefore, arsenic concentrations in silicate minerals are typically ~ 1mg/kg or less (Smedley and Kinniburgh, 2002). Many igneous and metamorphic rocks have average arsenic concentrations of 1-10 mg/kg. Similar concentrations are found in carbonate minerals and carbonate rocks (Plant *et al*, 2004).

2.3 Sources of Arsenic

2.3.1 Natural sources of arsenic

Arsenic is a component of more than 245 minerals. Arsenopyrite also unofficially called mispickel (FeAsS) is the most common arsenic-bearing mineral. On roasting in air, the arsenic sublimes as arsenic (III) oxide leaving iron oxides. The most important compounds of arsenic are arsenic (III) oxide, As_2O_3, ("white arsenic"), the yellow sulfide orpiment (As_2S_3) and red realgar (As_4S_4), Paris green, calcium arsenate, and lead hydrogen arsenate. The latter three have been used as agricultural insecticides and poisons. Orpiment and realgar were formerly used as painting pigments, though they have fallen out of use due to their toxicity and reactivity. Although arsenic is sometimes found native in nature, its main economic source is the mineral arsenopyrite mentioned above; it is also found in arsenides of metals such as silver, cobalt (cobaltite: CoAsS and skutterudite: $CoAs_3$) and nickel, as sulfides, and when oxidized as arsenate minerals such as mimetite, $Pb_5(AsO_4)_3Cl$ and erythrite, $Co_3(AsO_4)_2$. $8H_2O$, and more rarely arsenites ('arsenite' = arsenic (III), AsO_3^{3-} as opposed to arsenate (V), AsO_4^{3-}).

2.3.2 Anthropogenic arsenic

In 2005, China was the top producer of white arsenic with almost 50% world share, followed by Chile and Peru, reports the British Geological Survey.

2.4 Chemistry of Arsenic

2.4.1 Chemical properties of arsenic

Arsenic is a chemical element in the nitrogen family (group VA of the Periodic Table), existing in both gray and yellow crystalline forms. It is widely distributed in nature, and occasionally found uncombined, usually in association with such metals as antimony and silver. It also occurs combined in its sulfides realgar and orpiment; as arsenic oxide; and as a constituent of various metallic sulfides, of which arsenopyrite is the most abundant. Although some forms of arsenic are metal-like, it is best classified as non-metal. The chemical properties are given in table 2.1.

Table 2.1 Chemical Properties of Arsenic (Encyclopedia Britannica, 1994)

Parameter	Value
Atomic number	33
Atomic weight	74.92158
Melting point (gray form)	814°C (1,497°F) at 36 atmospheres pressure
Density (gray form) (yellow form)	5.73 g/cc at 14°C (57°F) 2.03 g/cc at 18°C (64°F)
Boiling point	616°C (1141°F) (sublimes)
Specific gravity (α,β,γ)	2.026, 4.7, 5.727
Oxidation number	-3, 0, +3, +5
Electrical configuration	2-8-18-5 $1s^2 2s^2 2p^6 3s^2 3p^6 3d^{10} 4s^2 4p^3$
Electrical resistivity	33.3μohm cm (273 K)
Covalent radius	121 pm
Ionic radius (As^{3+})	69 pm
Metallic radius	139 pm
Toxicity level	0.5 $mg.m^{-3}$ of air

2.4.2 Chemistry of arsenic in water

Arsenic is stable in four oxidation states (+5, +3, 0, -3). The oxidation state is closely related to the arsenic immobilization and hence the release of arsenic from its geological formations into the water bodies and biosphere (Dahi, 1997). Both the oxidation state and the release are determined by the soil and water pH, the redox potential, the in excess occurrence of sulfide, the occurrence of other ions as well as solids of especially iron and manganese (Dahi, 1997). In reducing waters, arsenic is found primarily in the trivalent form [As (III)] and forms arsenous acid. Arsenic (V) forms arsenic acid. Arsenous and arsenic acid dissociate to form respectively arsenite and arsenate ions. Table 2.2 shows the reactions that governs the speciation of arsenic and their equilibrium constants.

Table 2.2 Chemical equilibria of arsenic and arsenious acid (Cherry, 1979)

Arsenic acid:				
$H_3AsO_4 + H_2O$	=	$H_2AsO_4^-$	$+ H_3O^+$	pKa = 2.20
$H_2AsO_4^- + H_2O$	=	$H AsO_4^{2-}$	$+ H_3O^+$	pKa = 6.97
$H AsO_4^{2-} + H_2O$	=	AsO_4^{3-}	$+ H_3O^+$	pKa = 11.53
Arsenious acid:				
$H_3AsO_3 + H_2O$	=	$H_2AsO_3^-$	$+ H_3O^+$	pKa = 9.22
$H_2AsO_3^- + H_2O$	=	$H AsO_3^{2-}$	$+ H_3O^+$	pKa = 12.13
$H AsO_3^{2-} + H_2O$	=	AsO_3^{3-}	$+ H_3O^+$	pKa = 13.40

2.5 Acute Arsenic Toxicity in Human

Acute arsenic exposures (high concentrations ingested over a short time period) can cause a variety of adverse effect. The severity of the effect depends primarily on the level of exposure. Acute high-dose oral exposure to arsenic typically leads to gastrointestinal irritation accompanied by difficulty in swallowing, thirst, abnormally low blood pressure and convulsions. Death may occur from cardiovascular collapse. The respiratory tract, nervous system, skin may be considered as the critical targets of

prolonged arsenic exposures. Prolonged arsenic toxication results are shown in the Table 2.3.

Table 2.3 Arsenic Poisoning From Drinking Water	
Main organ	Effects
Nervous system disorders	Ataxia, paralysis, peripheral neuropathy
Respiratory system distress	Nasal septum perforation, bronchitis and cancer
Skin changes	Melanosis, dermatitises, hyperkeratosis and cancer
Heart	Heart and occlusive arterial disease
Liver	Liver cirrhoses and cancer

Arsenic-contaminated groundwater, used as drinking water, has been a severe problem in Bangladesh but is also common in United States (Bissen and Frimmel, 2003). Several studies have reported the health hazard due to the chronic exposure to arsenic. The standards for maximum concentrations of arsenic in drinking water have been declining since the high toxicity of arsenic has become apparent. The 1903 report of the Royal Commission on Arsenic Poisoning in the UK set a standard of 150 μg/l. In 1942, the US Public Health Service set a drinking water standard of 50 μg/l for interstate water carriers. The World Health Organization (WHO) guideline value and the European maximum permissible concentration (MPC) for arsenic in drinking water are set as 10 μg/l. The United States Environmental Protection Agency (EPA, 2005) also lowered the drinking water standard for arsenic from 50 to 10 μg/l starting January, 2006. Most western countries adopted this limiting their current drinking water standards (Yamamura, 2003). On the other hand, many affected countries like Bangladesh still operate 50μg/l standard due to lack of adequate testing facilities.

2.6 Conventional Arsenic Removal Technologies

2.6.1 General

A variety of technologies has been used for removal of arsenic from water. The most common technologies to remove arsenic are precipitation/sedimentation, co-precipitation and adsorption onto coagulation flocs, filtration, adsorption onto activated carbon, Fe-Mn oxidation, and lime softening. For all of these technologies (except reverse osmosis) adsorption is the fundamental process governing arsenic removal (Holm, 2002). The current advanced treatment options to remove arsenic include activated alumina, iron-oxide-coated-sand, reverse osmosis, ion exchange, and electro-dialysis. The following sections briefly describe some of the arsenic removal technologies.

2.6.2 Alum and iron flocculation process

Arsenic can be effectively removed by coagulation using alum; ferric salts etc. (Holm, 2002). Ferric salts have been found to be more effective in removing arsenic than alum on a weight basis and effective over a wider range of pH (Holm, 2002). In both cases, pentavalent arsenic (arsenate) can be more effectively removed than trivalent arsenic (arsenite). These products might form through precipitation, co-precipitation or adsorption mechanisms. Precipitation refers to the insolubilization of contaminants by exceeding solubility products, in this case of either $FeAsO_4$ or $AlAsO_4$ solids. Co-precipitation is defined as an incorporation of soluble arsenic species into a growing hydroxide phase via inclusion, occlusion, or adsorption. Finally, adsorption refers to formation of surface complexes between soluble arsenic and the solid oxyhydroxide surface site.

In the coagulation-flocculation process aluminum sulfate or ferric chloride or ferric sulfate is added and dissolved in water under efficient stirring for one to few minutes. Rapidly aluminum or ferric hydroxide micro flocs are formed. The water is then gently stirred for few minutes for agglomeration of micro flocs into larger easily settleable flocs. During this flocculation process all kinds of micro particles and

negatively charged ions are attached to the flocs by electrostatic and chemical attachment. Arsenic is also adsorbed onto coagulated flocs. As trivalent arsenic occurs in non-ionized form; it is not subjected to significant removal. Oxidation of As(III) to As(V) is thus required to a pretreatment step for efficient removal. This can be achieved by addition of bleaching powder (chlorine) or potassium permanganate. Arsenic adsorbed on ferric hydroxide flocs as Fe-As complex is removed by sedimentation. Filtration may be required to ensure complete removal of all flocs. Similar reaction take place in case of alum with the formation of Al-As complex as an end product which is removed by the process of sedimentation and filtration.

2.6.3 Passive sedimentation

Passive sedimentation received considerable attention because of rural people's habit of drinking stored water from pitchers. Oxidation of water during collection and subsequent storage in houses may cause a reduction in arsenic concentration in stored water. Experiments conducted in Bangladesh showed zero to high reduction in arsenic content by passive sedimentation. Arsenic reduction by plain sedimentation appears to be dependent on water quality particularly the presence of precipitating iron in water. It is found that more than 50% reduction in arsenic content is possible by sedimentation of tube-well water containing 380-480 mg/L of alkalinity as $CaCO_3$ and 8-12 mg/L of iron but cannot be relied to reduce arsenic to desired level (Ahmed *et al.*, 2000). Most studies showed a reduction of zero to 25% of the initial concentration of arsenic in groundwater. In rapid assessment of technologies passive sedimentation failed to reduce arsenic to the desired level of 50 µg/L in any well (BAMWSP, DFID, Water-Aid, 2001).

2.6.4 Activated alumina

Activated alumina, Al_2O_3, having good sorptive surface is an effective medium for arsenic removal. Some of the activated alumina based sorptive media used in Bangladesh include:

- BUET Activated Alumina
- Alcan Enhanced Activated Alumina
- ARU of Project Earth Industries Inc., USA
- Apyron Arsenic Treatment Unit

The BUET and Alcan activated alumina have been extensively tested in field condition in different areas of Bangladesh under rapid assessment and found very effective in arsenic removal (BAMWSP, DFID, Water-Aid, 2001). The Arsenic Removal Units (ARUs) of Project Earth Industries Inc. (USA) used hybrid alumina and composite metal oxides as adsorption media. The Apyron Technologies Inc. (ATI) also uses inorganic granular metal oxide based media that can selectively remove As(III) and As(V) from water. The Aqua-Bind^{TM} arsenic media used by ATI consist of non-hazardous aluminium oxide and manganese oxide for cost-effective removal of arsenic.

2.6.5 Activated carbon

Removal of As(V) by adsorption onto activated carbon is more effective than that of As(III). Activated carbon is manufactured from carbonaceous material such as wood, coal, petroleum residue, etc. A char is made by burning the material in the absence of air. The char is than oxidized at high temperature to create a very porous structure. Activated carbon is crushed into granules ranging from 0.1 to 2 mm in diameter or is pulverized to a very fine powder. Dissolved materials are adsorbed to both exterior and interior surfaces of the carbon. When these surfaces become saturated with dissolved substances, the carbon must be regenerated. Design of granular-activated-carbon systems is based on flow rates and contact times. Carbon columns can be arranged in parallel to increase the capacity and in series to increase the contact time. The major problem associated with granular-activated-carbon-contact systems is plugging of the bed by suspended solids in the water.

2.6.6 Iron oxide coated sand

Iron oxide coated sand has been successfully employed in fixed beds to treat metal bearing wastewater (Subramanian, 2004). Iron oxide-coated sand showed promise as a medium for use in small systems or home treatment units in some developing areas of the world for removing As (III) and As (V). Iron oxide coated sand is prepared by washing and drying river sand and then mixing it with ferric nitrate solution. Water is passed through the column with sufficient contact time and arsenic is adsorbed on iron oxide coated sand. The medium is regenerated by sodium hydroxide solution. Iron oxide coated sand is a low cost and simple process for use in small systems or home treatment units in developing areas of the world.

2.6.7 Ion exchange

Ion exchange is usually used to demineralize, to soften and to de-nitrate water. During treatment ion exchange involves the reversible exchange of ions between a solution and a solid phase that are in direct contact (Rubel, 2003 (b)). The solid phase can be natural zeolite or a synthetic resin consisting of a cross linked polymeric network with charged ionic species that retain them by electrostatic forces. Resins exhibit affinity to all ionic species of opposite charge, depending upon the specific ionic charge, the hydrated ionic radius, the concentration in solution, and the degree of resin cross-linking and the nature of the functional group on the resin (e.g., sulphonic, phosphonic or carbonic acid groups). For arsenic removal, an ion-exchange resin, usually loaded with chloride ions at the "exchange sites", is placed in vessels (Mittal, 2002). The arsenic containing water is passed through the vessels and the arsenic exchanges for the chloride ions.

Arsenic exchange (R = Resin):

$$2R\text{-}Cl + HAsO_4^{2-} = R_2AsO_4 + 2Cl^-$$

Regeneration:

$$R_2AsO_4 + 2Na^+ + 2Cl^- = 2R\text{-}Cl + HAsO_4^{2-} + 2Na^+$$

As ion exchanged is effective only in removing ions from the water, only As(V) which is present in ionic form in the neutral pH range (the pH range of most natural water) can be exchanged in resins. So the efficiency of the ion exchange process can be improved by pre-oxidation of As(III) to As(V).

2.6.8 Membrane techniques

Demineralization of water can be accomplished using micro-porous membrane. There are two basic modes of operation in use. One system uses pressure to drive water through the membrane against the force of osmotic pressure and is called reverse osmosis, even though the pressure applied is several orders of magnitude in excess of the natural osmotic pressure. The other process, called electro-dialysis uses electrical forces to drive ions through ion-selective method.

2.6.9 Microbial process

Microbial removal of arsenic is based on two important metal-microbe interactions: (i) microbial oxidation of As(III) to As(V) to facilitate its removal by conventional arsenic removal processes and (ii) bioaccumulation of arsenic in bacterial biomass from the surrounding water environment. There are a number of microorganisms capable of oxidizing arsenite at neutral pH. The common iron bacteria which oxidize ferrous iron to ferric iron can oxidize, as well as absorb arsenic. Removal of trace metal from water through accumulation in algae is well recognized. Several forms of algae are known to assimilate arsenic from water in a biological process. Arsenic can conventionally be oxidized from As(III) to As(V), adsorbed or assimilated through microbial growth in a simple reactor in nutritionally balanced condition at appropriate temperature and pH and subsequently removed by precipitation/filtration. Microbial growth on fixed media or suspended growth should be equally effective for arsenic removal.

2.7 Adsorption Isotherms

2.7.1 General

An adsorption isotherm specifies the equilibrium surface concentration of adsorbate on adsorbent as a function of bulk concentration of adsorbate in solution. It is called isotherm because it describes the equilibrium state of adsorbate, adsorbent, and solute at a given temperature.

2.7.2 Langmuir isotherm

The Langmuir isotherm was developed by Irving Langmuir in 1916 to describe the dependence of the surface coverage of an adsorbed gas (or adsorbate in aqueous solutions) on the pressure (or concentration) of the gas (or adsorbate) above the surface at a fixed temperature. There are many other types of isotherm (BET, Freundlich) which differ in one or more of the assumptions made in deriving the expression for the surface coverage; in particular, on how they treat the surface coverage dependence of the enthalpy of adsorption. Whilst the Langmuir isotherm is one of the simplest, it still provides a useful insight into the pressure dependence of the extent of surface adsorption. The Langmuir Adsorption Isotherm describes equilibrium between surface and solution as a reversible chemical equilibrium between species (Langmuir, 1918). The adsorbate surface is considered to be made up of fixed individual sites where molecules of adsorbate may be chemically bound. Denoting an unoccupied surface site as (–*S*) and the adsorbate in dilute solution as species (*A*), with concentration (*C*), and considering reaction between the two to form occupied sites (-*SA*):

$$-S + A \rightleftharpoons -SA$$

Assuming that this reaction has a fixed free energy of adsorption equal to $\Delta G°a$ that is not dependent on the extent of adsorption and not affected by interaction among sites. Each site is assumed to be capable of binding at most one molecule of adsorbate; the Langmuir model allows accumulation only up to a monolayer.

In practice, the actual number of sites per surface area and the energy of adsorption are usually unknown. Instead, the variable of interest is q, the number of moles of adsorbate per mass of adsorbent at equilibrium. The Langmuir equation transforms to

$$\frac{q}{Q} = \frac{bC}{1+bC}$$

where Q is the maximum number of moles adsorbed per mass adsorbent when the surface sites are saturated with adsorbate (i.e., a full monolayer), and b is an empirical constants with units of inverse concentration. The Langmuir Isotherm is shown in figure 2.1.

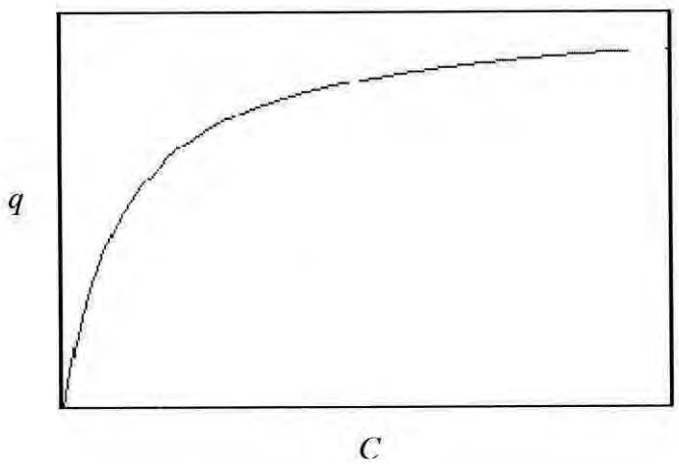

Figure 2.1. Typical Langmuir Isotherm curve (Langmuir, 1918)

The Langmuir adsorption isotherm has found wide applicability to adsorption of compounds in water treatment. Its advantages include its simplicity, its foundation in a model with some physical basis, and its ability to fit a broad range of experimental data. Its limitations include (i) the assumption that the energy adsorption is independent of degree of coverage, (ii) reversibility of bonding, and (iii) allowance for at most only one monolayer. Mass adsorbed, q, is assumed to approach a saturating value, Q, when C becomes very large.

2.7.3 Brunauer-Emmett-Teller (BET) adsorption isotherm

The BET (Brunauer *et al.*, 1938) extends the Langmuir model from a monolayer to several molecular layers. Above the mono layer, each additional layer of adsorbate molecules is assumed to equilibrate with the layer below it; layers of different thicknesses are allowed to co-exist. The equilibrium for the adsorption on to the new layers is defined by the law of mass action as for the Langmuir model for the first layer. The process of sorbing a new layer of adsorbate on to old layers is assumed to be identical to the process of condensing adsorbate from solution to solid or liquid. The resulting isotherm has the form

$$\frac{q}{Q} = \frac{BC}{(Cs - C)[1 + (B - 1)(C/Cs)]}$$

where B is a dimensionless constant related to the difference in free energy between adsorbate on the first and successive layers and C_s is the saturation concentration of the adsorbate in solution. As C approaches C_s, q becomes infinite as adsorbate precipitates on to surface. The different types of BET adsorption isotherms are shown in figure 2.2 (Sing *et al.*, 1985).

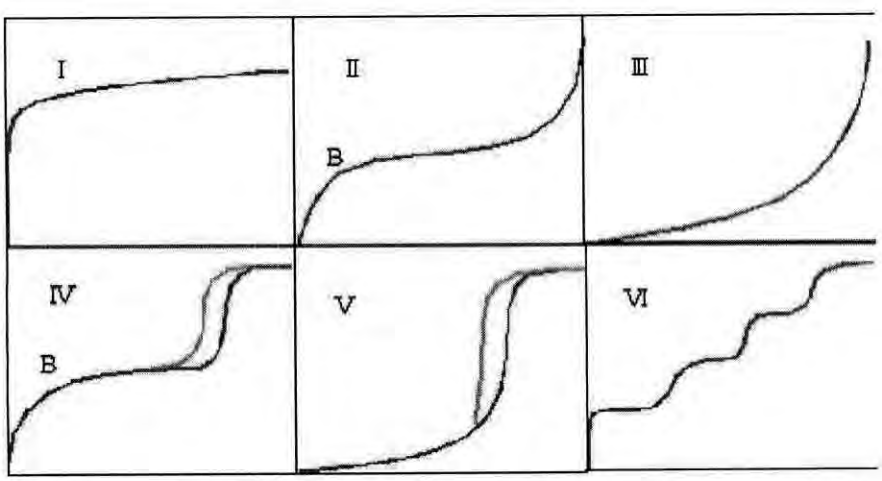

Figure 2.2. Types of BET adsorption isotherms (Sing *et al.*, 1985)

The Type I isotherm is typical of micro porous solids and chemisorption isotherms. Type II is shown by finely divided non-porous solids. Type III and Type V are typical

of vapor adsorption (i.e. water vapor on hydrophobic materials). Type IV and Type V feature a hysteresis loop generated by the capillary condensation of the adsorbate in the mesopores of the solid. Finally, the rare Type VI step-like isotherm is shown by nitrogen adsorbed on special carbon.

2.7.4 Freundlich isotherm

The Langmuir and BET models incorporate an assumption that the energy of adsorption is the same for all surface sites and not dependent on degree of coverage. In reality, the energy of adsorption may vary because real surfaces are heterogeneous. The Freundlich Adsorption Isotherm (Freundlich, 1926) attempts to account for this assuming that the frequency of sites associated with a free energy of adsorption decreases exponentially with increasing free energy. The isotherm will have the following form

$$q = aC^{1/n}$$

where a is a constant. Here the surface concentration of adsorbate does not approach a saturation value as C increases, since there are always surface sites with higher free energies of adsorption to fill. The Freundlich isotherm is very widely used to fit observed data empirically even when there is no basis for its underlying assumptions. A typical Freundlich adsorption isotherm is shown in figure 2.3.

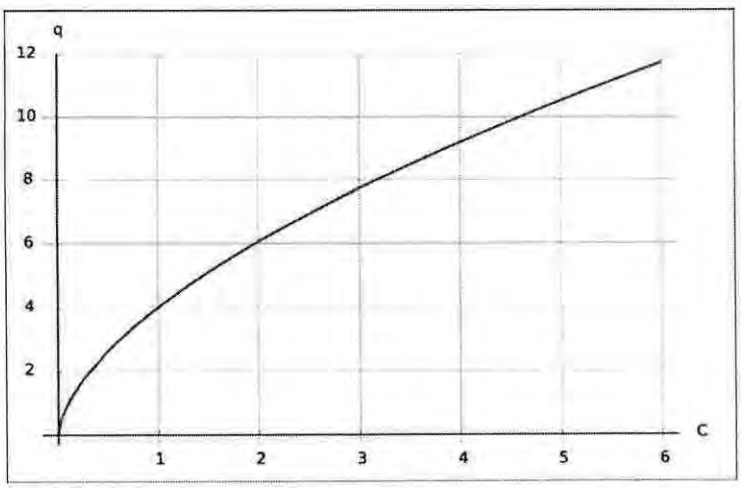

Figure 2.3. Typical Freundlich adsorption isotherm (Freundlich, 1926)

The adsorption characteristics of arsenic discussed in Section 4.3.1 showed, for MNPs, the maximum adsorption capacity (q_{max}) of arsenite was more than that of arsenate. However, a more in-depth analysis of the adsorption isotherms for both arsenite and arsenate is needed for better understanding of the adsorption phenomenon.

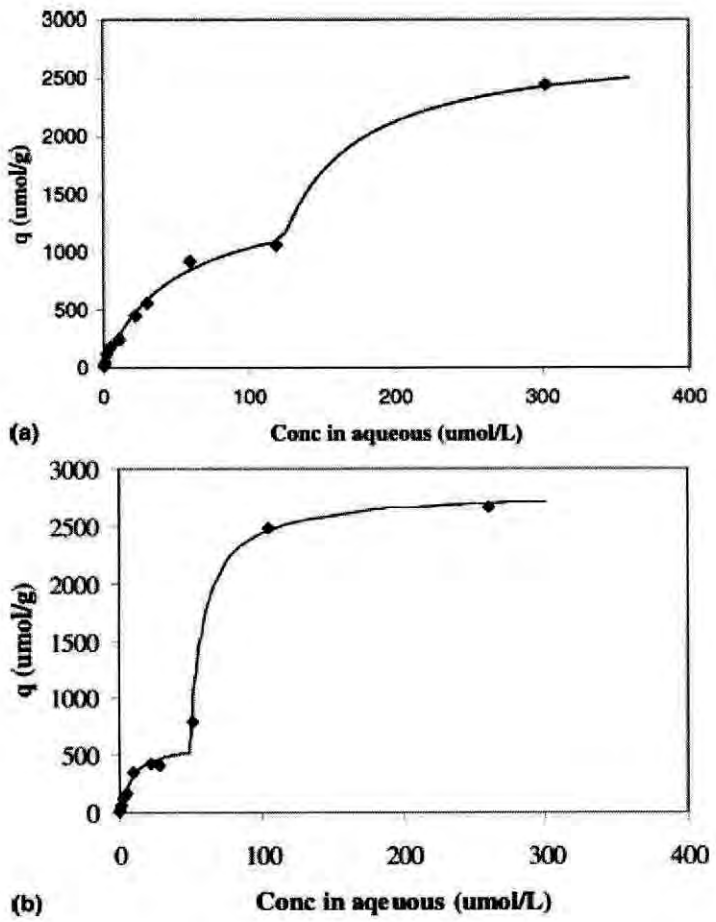

Figure 2.4. Adsorption of Arsenic to 11.72 nm magnetite at pH 8.0: (a) As(III) and (b) As(V) (Yean *et al.*, 2005)

2.8 Adsorption Kinetics

The kinetics of sorption describes the solute uptake rate, which in turn governs residence time or sorption reaction. It is one of the important characteristics in defining the efficiency or sorption. The kinetics of adsorption of any sorbate on a sorbent can be described by the pseudo first-order and second-order kinetic models. The first-order kinetic model (Lagergren, 1898) and the second-order kinetic model (McKay and Ho, 1999) are expressed as follows:

$$\log(q_e - q) = \log q_e - \frac{k_1 t}{2.303} \quad \text{..... (First-order kinetic model)}$$

$$\frac{t}{q} = \frac{1}{k_2 q_e^{\,2}} + \frac{t}{q_e} \quad \text{..... (Second-order kinetic model)}$$

Where, q_e and q (μM) are the amounts of sorbate (e.g. like As) adsorbed onto adsorbent at equilibrium and at time t, respectively. k_1 (hr^{-1}) and k_2 ($\mu M^{-1}\ hr^{-1}$) are the rate constants of first-order and second-order adsorption. The slopes and intercepts of plots of $\log(q_e - q)$ *versus* t were used to determine the first-order rate constant k_1 and q_e. The slopes and intercepts of plots of t/q *versus* t were used to calculate the second-order rate constant k_2 and q_e.

Chapter 3

CHARACTERIZATION OF MAGNETITE NANOPARTICLES

3.1 Introduction

Nanoparticles in the size range of 1~100 nanometer (nm) have attracted great attention to the researchers in recent times. Nanomaterial behavior may not be predictable from observations on larger-sized materials since nanomaterials might have different physical, chemical, and biological properties. Little is known about the characteristics of nanomaterials (e.g., particle size, aggregation, surface charge etc.). Meanwhile in recent research it has been observed that arsenic has a close chemical attraction with iron. So, the characteristics (size distribution, specific surface area, aggregation characterization, structure and composition, surface charge characteristics) of iron nanomaterial in order to find its suitability in arsenic removal system need to be determined. The commercially manufactured magnetite (Fe_3O_4) nanoparticle has been procured for characterization from Nanostructured & Amorphous Materials, Inc. 16840, Clay Road, Suite113, Houston, TX 77084, USA.

The available methods those were used in characterizing magnetite nanoparticle are X-ray Diffraction (XRD) for structure and composition, Brunauer-Emmett-Teller (BET) Method for surface area measurement, Dynamic Light Scattering (DLS) analysis for particle size distribution and Potentiometric Titration for surface charge characteristics.

This Chapter categorically describes the nanoparticle characteristics by different methods stated earlier in experimental basis. The laboratory test results were compared and checked with the properties provided by the manufacturer.

The details of magnetite nanopowder are given below which are provided by the manufacturer.

Table-3.1. Details of Commercially Procured Magnetite Nanoparticles	
Iron Oxide (Fe_3O_4)	
Purity:	98+ %
Apparent Particle Size (APS) :	20 - 30 nm
Specific Surface Area (SSA):	~ 60 m^2/g
Color:	black
Morphology:	spherical
Bulk density:	0.84 g/cm^3
True density:	4.8-5.1g/cm^3

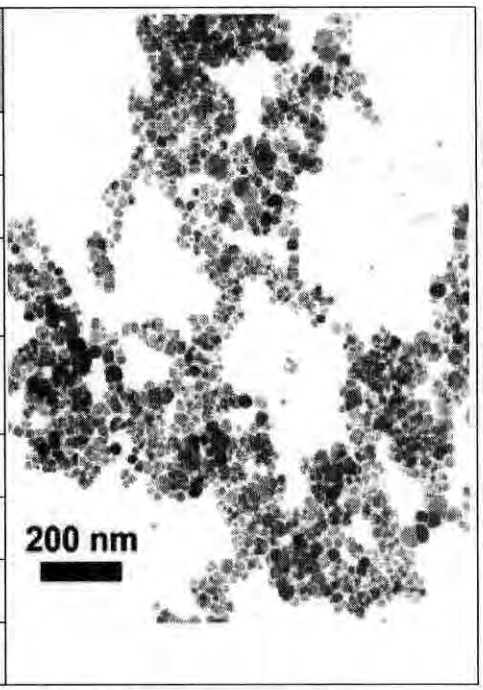

Figure 3.1. TEM image of 20-30 nm magnetites

(Source: Nanostructured & Amorphous Materials, Inc.
www.nanoamor.com/products)

3.2 Methodology for Characterization of Magnetite Nanoparticles

3.2.1 Surface area measurement by BET method

Physical gas adsorption is applied to study the pore characteristics of solid materials. The isotherm obtained from these adsorption measurements provides information on the Surface Area and Particle Size Distribution (PSD). Different probe gases including N_2, Ar, and CO_2 are frequently used as adsorptive, depending on the nature of the material (adsorbent) and the information required (Groen *et al.*, 2003). N_2 adsorption at 77 K (-196 °C) and at sub-atmospheric pressures has remained universally pre-eminent and can be used for routine quality control, as well as for investigation of new materials. If applied over a wide range of relative pressures

(p/p_0), N_2 adsorption isotherms provide information on size distributions in the micro, meso and macro-porosity range (approximately 0.5–200 nm). The classical pore size model developed by Barrett, Joyner and Halenda (BJH) in 1951, which is based on the Kelvin equation and corrected for multilayer adsorption (Barrett *et al.*, 1951).

BET (Brunauer-Emmett-Teller) method is base on physical adsorption of gas molecules on a solid surface .Effective surface area of the iron nanoparticles was estimated using Brunauer-Emmett-Teller (BET) physisorption method (Brunauer *et al.*, 1938). For the present study, Dr. Navid Bin Saleh (currently an Assistant Professor at University of South Carolina, USA) carried out the BET Surface Area analysis in the Laboratory of Yale University, where he worked as a Post-doctoral Research Associate. Nitrogen adsorption-desorption isotherms were measured at -196 °C using a static volumetric instrument Autosorb-1C (Quanta Chrome, Boynton Beach, FL). Prior to the measurement, the samples were out-gassed at 300 °C to a residual pressure of 5×10^{-3} Torr (5 mili-torr). The pore size distributions were estimated from the desorption isotherms using the BJH model (Barrett *et al.*, 1951).

3.2.2 Dynamic light scattering (DLS) analysis

Dynamic Light Scattering (DLS) is also known as Photon Correlation Spectroscopy. This technique is one of the most popular methods used to determine the size of particles. Shining a monochromatic light beam, such as a laser, onto a solution with spherical particles in Brownian motion causes a Doppler Shift when the light hits the moving particle, changing the wavelength of the incoming light. This change is related to the size of the particle. It is possible to compute the size distribution and give a description of the particle's motion in the medium, measuring the diffusion co-efficient of the particle and using the autocorrelation function. This method has several advantages: first of all the experiment duration is short and it is almost all automatized so that for routine measurements an extensive experience is not required. Moreover, this method has modest development costs. Commercial "particle sizing" systems mostly operate at only one angle (90°) and use red light (675 nm). Usually in these systems the dependence on concentration is neglected. Using more sophisticated

experimental equipment (projector, short-wavelength light source); the methods can be not only considerably extended, but also more complicated and expensive.

For the present study, Dr. Navid Bin Saleh carried out the DLS analysis in the Laboratory of Yale University, where he worked as a Post-doctoral Research Associate.

For DLS Analysis stock solution of the magnetite nanoparticle suspension was prepared in de-ionized water. Three test runs were made on magnetite samples. These consist of the following;

1) At first the particle size of magnetite was observed in de-ionized water after sonicating for 10 minutes.
2) Aggregation of the nanoparticles was observed after adding 10mM $NaNO_3$ in the solution as background electrolyte to commence aggregation.
3) Aggregation of the nanoparticles was observed after adding 10mM $NaNO_3$ and 50mM MES or HEPES in the solution to commence aggregation.

The aggregation experiments were performed using a multi-angle light scattering unit (ALV-5000, Langen, Germany) equipped with a solid-state Nd:vanadate ($Nd:YVO_4$) laser (Verdi V2, Coherent, Santa Clara, CA) providing a single-frequency output of 532nm. Further details of the instrument are described elsewhere (Chen and Elimelech, 2007). The iron nanoparticle samples were placed in new glass vials (Supelco, Bellefonte, PA) that were previously soaked in a cleaning solution (Extran MA 01, Merck KGaA, Darmstadt, Germany) overnight, thoroughly rinsed in deionized water, and oven-dried under dust-free conditions(Saleh *et al.*, 2008). Electrolyte solutions, pH adjusting reagents, and biological buffers were added prior to the aggregation experiments following the protocol described by Chen and Elimelech (Chen and Elimelech, 2006; Chen *et al.*, 2006). The dynamic light scattering measurements were conducted by positioning the detector at 90° with the incident laser beam and the autocorrelation function having been allowed to accumulate for over 15 s. The measurements were performed for a time period ranging from 20 min to 3 h to obtain an approximately 30% increase in the original

hydrodynamic radius of the iron nanoparticles while these experiments were carried out at room temperature (23 °C).

The early-stage aggregation kinetics are expressed as the initial rate of increase in the hydrodynamic radius $a_h(t)$ with time t, as measured by DLS. This increase in $a_h(t)$ is linearly dependent on the initial (primary) particle concentration,N_0, as well as the initial aggregation rate constant, K_{11} (Eq. 3.1) (Mylon *et al.*, 2004; Chen *et al.*, 2006).

$$\left(\frac{da_h(t)}{dt}\right)_{t\to 0} \propto k_{11}N_0 \quad \ldots \quad \ldots \quad \ldots \quad (3.1)$$

3.2.3 X-ray diffraction analysis

X-ray Powder Diffraction (XRD) is an efficient analytical technique used to identify and characterize unknown crystalline materials. Monochromatic x-rays are used to determine the inter-planar spacing of the unknown materials. Samples are analyzed as powders with grains in random orientations to ensure that all crystallographic directions are "sampled" by the beam. When the Bragg conditions (specular reflection from crystal planes) reflection from for constructive interference are obtained, a "reflection" is produced, and the relative peak height is generally proportional to the number of grains in a preferred orientation.

The X-ray spectra generated by this technique, thus, provide a structural fingerprint of the unknown. Mixtures of crystalline materials can also be analyzed and relative peak heights of multiple materials may be used to obtain semi-quantitative estimates of abundances.

When crystallites are less than approximately 1,000 Å in size, appreciable broadening in the X-ray diffraction lines will occur. These regions may in fact correspond to the actual size of the particles. The approximate size of the nanoparticles can be found by Scherrer's equation.

In this research work the XRD analysis of the procured magnetite nanoparticle was performed at the Laboratory of Bangladesh Atomic Energy Commission (BAEC) to

analyze the composition of the magnetite nanoparticles. The XRD analysis was conducted with a *Philips X'Pert Pro X-ray Diffractometer* at 40kV and 30mA. It used copper Kα (CuKα) radiation and a graphite monochromator to produce X-rays with a wavelength of 1.54060 Å. Magnetite nanoparticles were placed in a 10mm specimen length and scanned from 15° to 70°. This scan range covered all major species of iron and iron oxides. The scanning rate was set at 2.0°/min (Step Size, 2Θ = 0.02, Scan Step Time, sec = 0.60).

3.2.4 Potentiometric titration

Potentiometric titrations of magnetite suspensions were carried out in 0.01, 0.05 and 0.1 M $NaNO_3$ as the background electrolytes. The concentration of magnetite nanoparticles was fixed at 0.5 g/L. Standard (0.05 M) acid (HCl) and base (NaOH) solutions were used for titration. After adding acid or bases, about 5 mins of slow and steady stirring was performed before measuring pH of the solution. The pH and corresponding acid or base additions were recorded.

The experimental protocol for titration consisted of the following steps: (i) First, stock solution of $NaNO_3$ (concentration: 1.0 M) was prepared. (ii) The aqueous solutions were prepared by adding required quantities (1 ml, 5 ml and 10 ml) of $NaNO_3$ stock solution in a 100 ml volumetric flask. (iii) The flask was filled with distilled water up to the 100ml mark. This way three different concentration of background electrolytes (0.01M, 0.05M and 0.10M) were prepared. After preparation of the final solution it was taken into a 150ml glass beaker. (iv) 0.05 g of magnetite nanoparticle was added in the required amount of solution to get a final concentration of 0.5 g/L of magnetite. (v) At the beginning of each experiment the magnetite nanoparticles were dispersed in solution by sonication using a sonication probe (Sonifier®, Branson Sonic Power Company Danbury, Connecticut, Power Supply, B-12.) for 10 min. (vi) After sonication the sample pH was measured and an equilibration period was allowed so that the pH value remained fixed for about one minute. (vii) Then required amount of 0.05M HCl or 0.05M NaOH solution was added to the solution using a micropipette and the suspension was stirred with a magnetic stirrer for about 10 minutes. (viii)

After that the solution pH was measured again in the same way as mentioned in step (vi). (ix) Step (vii) and (viii) were repeated consecutively until a pH range of 3 to 10 was obtained. For one concentration of background electrolyte, titration by 0.05M HCl and 0.05M NaOH were carried out in duplicate.

3.3 Results and Discussion

3.3.1 Specific surface area of magnetite nanoparticles

Figure 3.2 shows the adsorption isotherm of N_2 to the iron nanoparticles. The maximum N_2 adsorption occurs when partial pressure is close to unity and the value is about 260 cc/g of magnetite and about 100 cc/g of hematite. Regarding classification of physisorption isotherm, we find the Reversible Type-II isotherm where it represents unrestricted monolayer-multilayer adsorption (Sing *et al.*, 1985). Point B, the beginning of the almost linear middle section of the isotherm, found at Partial Pressure of 0.56 for magnetite and 0.60 for hematite, indicates the stage at which monolayer coverage is complete and multilayer adsorption is about to begin. The Type-II isotherm is amenable to the BET analysis, provided that the value of C is neither too low nor too high and that the BET plot is linear for the region of the isotherm containing Point B.

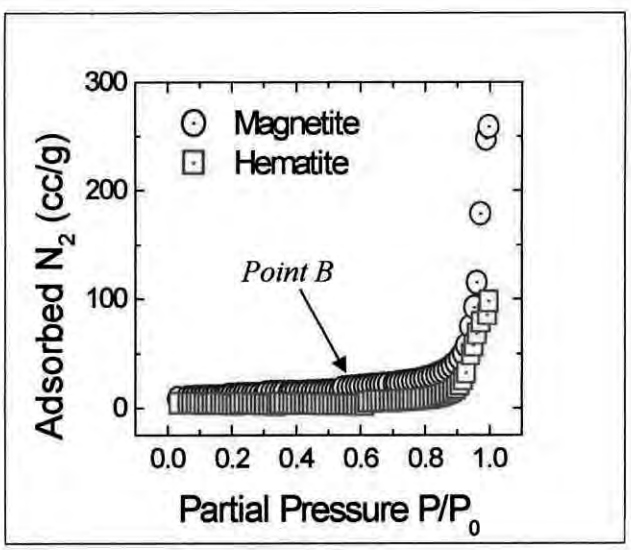

Figure 3.2. Adsorption isotherm of N_2 to the iron nanoparticles

The BET specific surface area measurement of the MNPs and HNPs were found to be 37.7 m^2/g and 13.8 m^2/g, respectively. This value for MNPs differs from that mentioned by the manufacturer (60 m^2/g). However, the surface area determined from test result is more acceptable than that reported by the manufacturer as surface area is determined by nitrogen gas adsorption to particles which was a direct measure for porous properties.

Figure 3.3 describes the pore size distribution of iron nanoparticles with the help of BJH model (Barrett *et al.*, 1951). From that figure, we find the internal pore size range of magnetite and hematite nanoparticles are about 15-28 °A and 18-30 °A, respectively. The internal pore diameter was found by desorbing N_2 gas from particle surfaces with the application of BJH model.

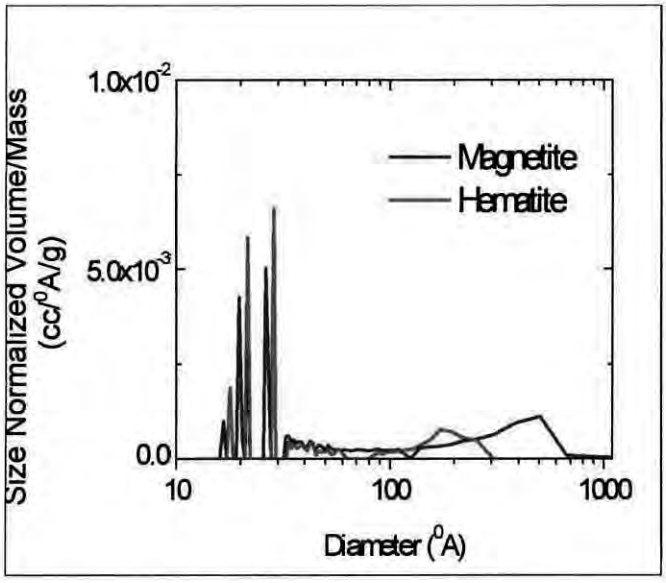

Figure 3.3. Pore size distribution of iron nanoparticles generated using BJH model while desorbing N_2 from particle surfaces

3.3.2 Structure and composition of magnetite nanoparticles

XRD measurements were conducted to identify the crystallographic structure of magnetite (Fe_3O_4) nanoparticles. The presence of Fe_3O_4 was indicated in XRD patterns as shown in Fig. 3.4. The peak (311) of the figure 3.4 was observed at

$2\theta \approx 36^{\circ}$. Thus it indicated that the formation of Fe_3O_4 nanoparticles was approximately 22.9 nm in mean diameter.

For a spherical particle the specific surface area (SSA) can be calculated by the following equation:

$$SSA = \frac{SurfaceArea}{Mass} = \frac{\pi d^2}{\rho \frac{\pi}{6} d^3} = \frac{6}{\rho d}$$

where ρ is the density (4800-5100 kg/m^3 for magnetite) of the solid particle. The theoretical SSA for 22.9 nm particles is therefore 51374-54585 m^2/kg or 51.374-54.585 m^2/g. However, the data obtained on surface area from the BET analysis (37.7 m^2/g) should be taken to be more precise, as in case of BET analysis the shape of the particle was not considered and surface area was determined on the basis of N_2 adsorption on the surface of magnetite nanoparticles.

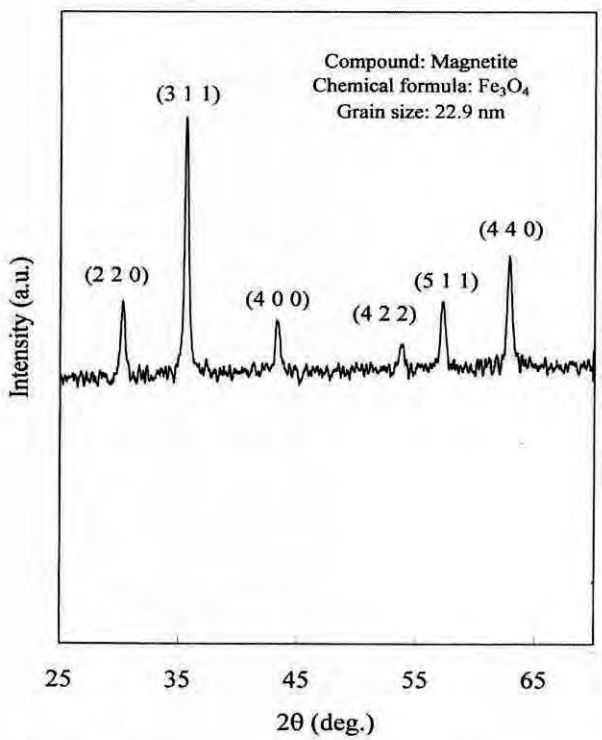

Figure 3.4. X-ray Diffraction (XRD) pattern of Magnetite Nanoparticles

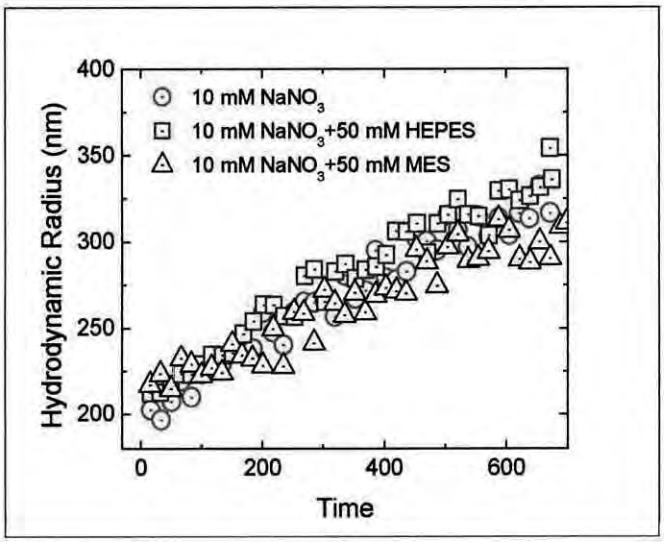

Figure 3.6. Aggregation profiles of magnetite nanoparticles with and without the biological buffers

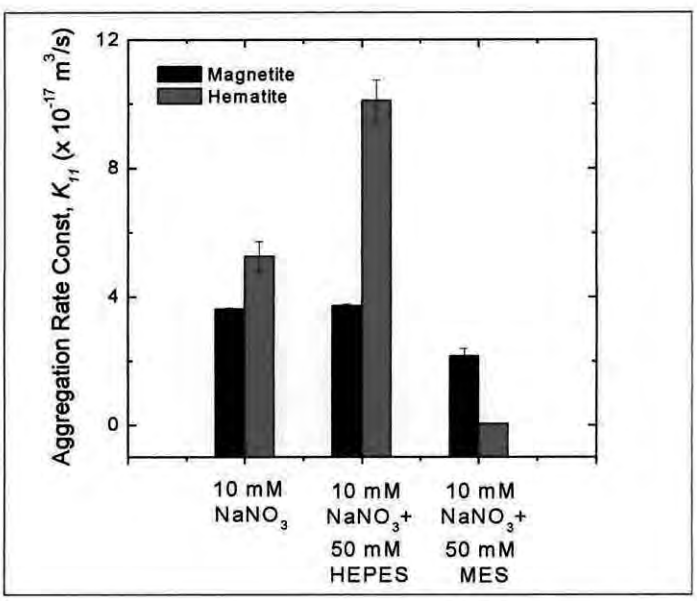

Figure 3.7. Aggregation rate constants of magnetite and hematite NPs with and without the biological buffers

3.3.3 Size distribution

Figure 3.5 shows the hydrodynamic radius for magnetite and hematite nanoparticles in aqueous suspensions. The concentration of the suspensions was 10 mg/l. The figure shows the average hydrodynamic radius of magnetite and hematite nanoparticles were fairly constant during the entire test and were measured as 193.1±5.7 nm and 62.1 ± 1.3 nm, respectively (Chen and Elimelech, 2006; Chen *et al.*, 2006).

The particle aggregation profiles for magnetite nanoparticle with and without biological buffers are shown in figure 3.6. Comparing with the figure 3.5, it is observed that aggregation increases with addition of background electrolyte such as $NaNO_3$. Here concentration of the electrolyte was 10 mM. After addition of 50 mM biological buffer solutions, we find no significant changes in hydrodynamic radius of the magnetite nanoparticles throughout the experiments. This aggregation may be a result of the promotion of double layer compression. The aggregation rate constants (K_{11}) for magnetite and hematite nanoparticles with and without biological buffers are shown in figure 3.7. The rate constant remains almost same for MNPs but it changes for HNPs with and without addition of buffers in $NaNO_3$ electrolyte. The aggregation rate constants are calculated based on initial aggregation of nanoparticles.

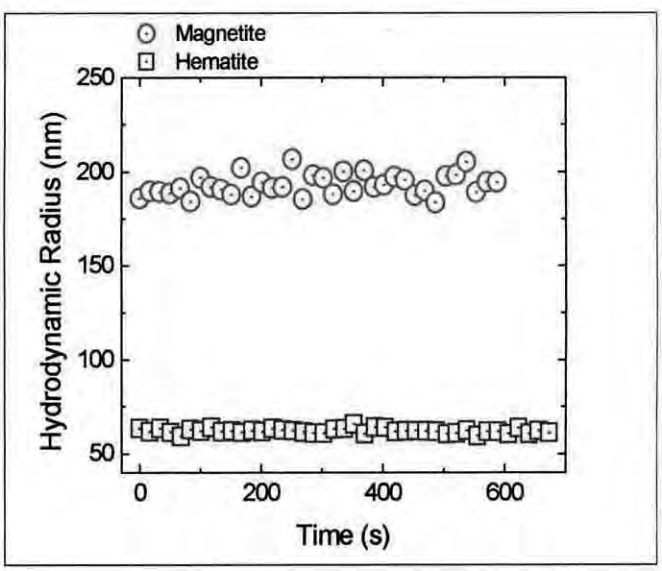

Figure 3.5. Hydrodynamic Particle Sizing of Magnetite and Hematite Nanoparticles

3.3.4 Surface charge characteristics

The pH versus surface charge (σ) data for 0.5 g/L magnetite suspension is plotted in Fig. 3.8. The surface charge (σ) was calculated as a function of pH from potentiometric titration data according to Eq. 3.2 (Stumm and Morgan, 1995).

$$\sigma(C\,m^{-2}) = F(C_A - C_B + [OH^-] - [H^+])a^{-1}S^{-1} \quad \ldots \quad \ldots \quad (3.2)$$

where F is the Faraday constant (96,485 C/mol), C_A and C_B are the total concentrations of acid and base added, respectively (mol/L), $[H^+]$ is the proton concentration (mol/L) given by $10^{-pH}/\gamma_{H^+}$, $[OH^-]$ is the OH^- concentration (mol/L) given by $10^{-(pKw-pH)}/\gamma_{OH^-}$, a is magnetite concentration (g/L), and S is the specific surface area (m^2/g). The titration curves (Fig. 3.8) are normalized to unit surface area. The point of zero surface charge (pH_{pzc}) is defined as the pH value at which σ=0. From the titration curve we find that the magnetite samples for all the three ionic suspensions (0.01, 0.05 and 0.10 M of $NaNO_3$) have the same pzc (pH of zero particle surface charge) values of pH 7.0. The result of pzc obtained in this research is close to those from the literature which is 6.6 (experimentally determined) (Tewari and McClean, 1972; Marmier *et al.*, 1999). Choudhury (2009) found pH_{pzc} of hematite nanoparticles to be 6.5.

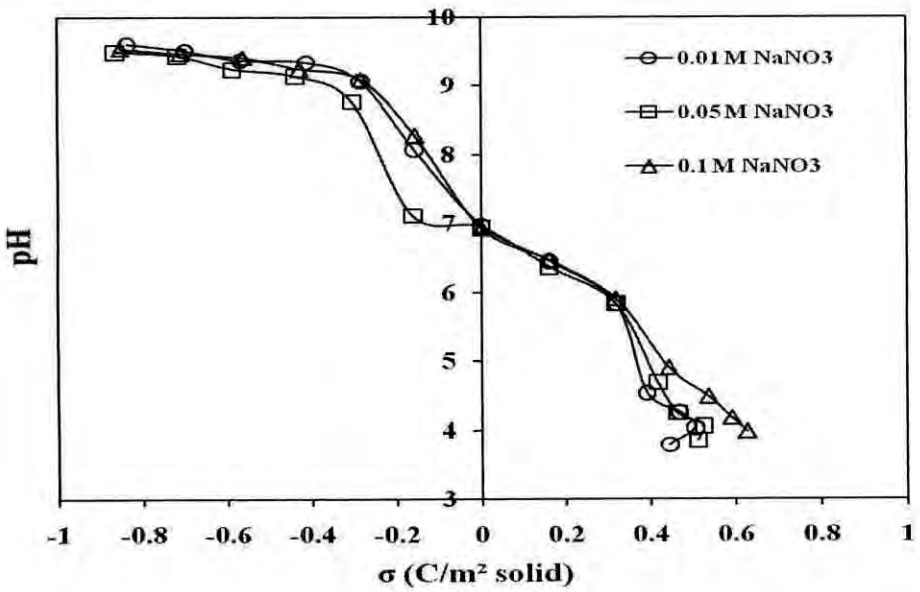

Figure 3.8. Potentiometric titration curves for surface charge (pH versus σ, C/m^2 solid)

The results indicate that there is a change of nanoparticle surface charge from positive to negative with the increase in pH values. This particular intrinsic surface charge property of magnetite nanoparticle has a very significant role in its adsorption characteristic. As arsenate remains negatively charged in aqueous solutions, therefore, high pH (>7.0) of the electrolyte will reduce the arsenate adsorptive capacity of magnetite nanoparticle where low pH (<7.0) increases the capacity. On the other hand, arsenite adsorption on magnetite nanoparticle is independent of the entire pH range as it is not charged in aqueous ionic solutions (Yean *et al.*, 2005). Figure 3.9 shows the potentiometric titration curve for total acid base addition in magnetite suspension at three different ionic strengths.

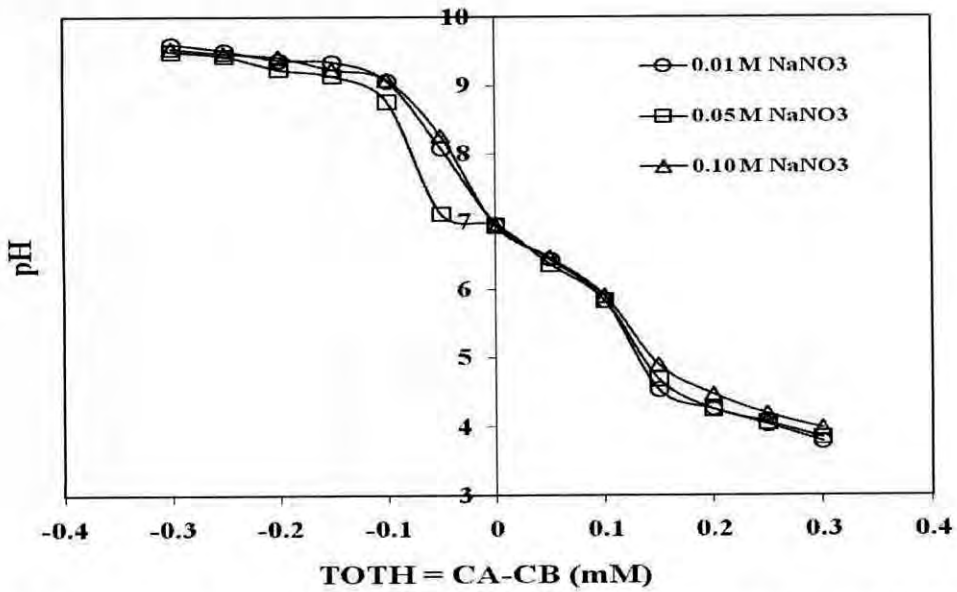

Figure 3.9. Potentiometric titration curves for total acid-base (pH versus TOTH, mM)

3.4 Summary

This chapter has discussed the characteristics of magnetite nanoparticles (MNPs) for a prominent adsorbent for removal of heavy metal like arsenic. There were specific determinations for characterization of MNPs such as specific surface area determination, structure, composition and size distribution of MNPs, surface charge characteristics. All the characteristics of magnetite nanoparticles play vital roles in adsorption of arsenic from water.

The specific surface area (SSA) of MNPs and HNPs found by BET adsorption isotherm method were 37.7 m^2/g and 13.8 m^2/g. This value for MNPs differs from that reported by the manufacturer ($60m^2/g$). The adsorption isotherm found by BET method holds the shape of Type-II, where it represents unrestricted monolayer-multilayer adsorption (Sing *et al.*, 1985). The pore size distribution was determined by BJH model (Barrett *et al.*, 1951). The internal pore size distribution for MNPs and HNPs ranges from 15-28°A and 18-30 °A, respectively.

The structure and composition of MNPs was assessed by X-ray diffraction analysis. This method gave the approximate mean diameter of magnetite nanoparticles which was 22.9 nm. With this size of particle the calculated specific surface area (SSA) was found around 51.4 to 54.6 m^2/g.

The characteristic of hydrodynamic radius (R_h) for MNPs and HNPs were conducted by Dynamic Light Scattering (DLS) analysis. The hydrodynamic radius of MNPs and HNPs were 193.1±5.7 and 62.1 ± 1.3 nm, respectively, in aqueous suspension. The hydrodynamic radius of MNPs increased in presence of background electrolyte ($NaNO_3$) with or without biological buffers and the radius increased almost 1.8 times of its initial hydrodynamic radius.

The surface charge characteristic of magnetite nanoparticles was a major finding for equilibrating experimental adsorption data. Potentiometric titration was conducted for this determination. The surface charge characteristic of MNPs is important in arsenic adsorption phenomenon in different pH values. The pH of zero surface charge (pH_{pzc}) for MNPs was 7.0 in this study.

Chapter 4

ADSORPTION OF ARSENIC ON MAGNETITE (Fe_3O_4) NANOPARTICLES

4.1 Introduction

A detailed assessment of adsorption characteristics of arsenic on magnetite under different conditions has been described in this chapter in an effort to evaluate its potential for use in arsenic removal systems. This chapter presents results of arsenic (both arsenate and arsenite) removal from groundwater by adsorption onto magnetite (Fe_3O_4) nanoparticles. The adsorption isotherms, adsorption envelopes, adsorption kinetics have also been evaluated in this chapter. In addition, assessment of the effect of phosphate (competing anion) is also presented.

4.2 Material and Methods

4.2.1 Batch adsorption experiments

Adsorption of Arsenic

Adsorption of arsenic and phosphate on magnetite nanoparticle (MNP) was assessed in batch experiments at both environmentally representative and higher concentrations. Aqueous solutions having arsenic concentrations ranging from 0 to 0.33 mmol/L (0 to 25 ppm) were equilibrated with known mass of magnetite nanoparticles. The concentration of MNP, with addition 0.005g MNP in a 50 ml centrifuged tube, was 0.1 g/L. The pH values of the batch tests were kept constant with biological buffers (e.g., MES, HEPES, and CHES) and required amount of 1.487 M NaOH. 2(N-Morpholino)-ethanesulfonate (MES), 4-(2-hydroxyethyl)-1-

piperazine-ethanesulfonate (HEPES), and 2-(cyclohexylamino) -ethanesulfonate (CHES) were added as buffers for fixing pH values of 5.15 and 6.1, 7.5, and 9.3 respectively.

The arsenic batch adsorption experiments consisted of the following steps: (i) Stock solutions of As(III) or As(V) (concentration:1000ppm), $NaNO_3$ (concentration: 1.0 M), MES or HEPES or CHES (concentration: 0.5 M) were prepared. (ii) Aqueous solutions were prepared by adding required quantities of arsenic (arsenite or arsenate) stock solution, 0.5 ml of $NaNO_3$ stock solution, 5.0 ml of biological buffer solution (MES for pH values of 5.15 and 6.1; CHES for pH values of 9.3; HEPES for pH values of 7.5) and required amount of 1.487 M NaOH in a 50 ml volumetric flask. (iii) The flask was filled with deionized water up to the 50ml mark. This way by changing the amount of arsenic stock solution, the arsenic concentration was varied from 0.1 ppm to 25.0 ppm and by changing the buffer and the amount of NaOH; the pH was kept constant at 5.15, 6.1, 7.5 and 9.3. (iv) The prepared aqueous solution was taken in a 50ml centrifuge tube and 0.005 g MNP was added to the solution; the resulting MNP concentration was 0.1 g/L. (v) At the beginning of each experiment the MNPs were dispersed in solution by sonication using a sonication probe (Sonifier(R), Branson Sonic Power Company Danbury, Connecticut, Power Supply, B-12.) for 10 min. (vi) The magnetite nanoparticle suspension in the centrifuge tubes was equilibrated in an end-over-end rotator [Fig. 4.1 (c)] for 24 hours at a constant speed of 20 rpm. (vii) After 24 hours the supernatant from the 50 ml centrifuge tubes were taken into 15 ml centrifuge tubes, and the 15 ml tubes were centrifuged for 10 minutes to settle the MNP to the bottom of the tube. (viii) The supernatant solutions were filtered through 0.2 μm Nalgene syringe filters (Surfactant Free Cellulose Acetate, SFCA). (ix) The pH of the supernatant was measured immediately after filtration. (viii) Arsenic concentration of the clear liquid collected from the tube was measured after suitably diluting the sample.

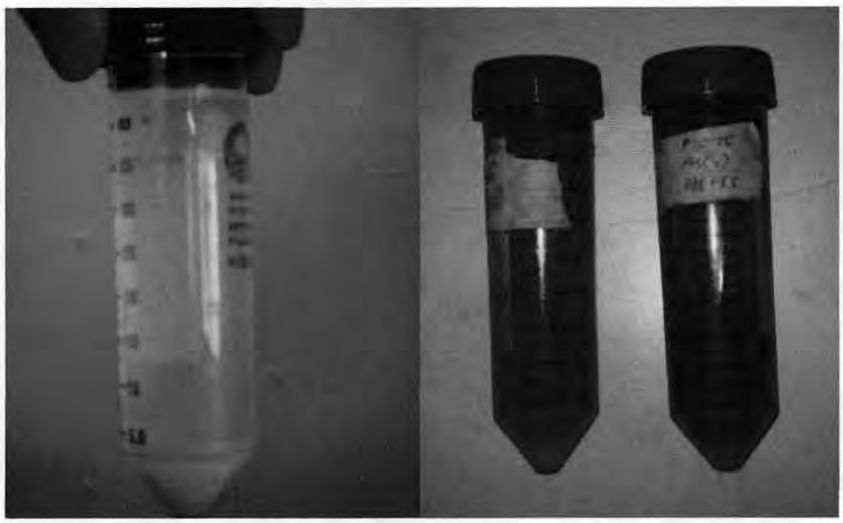

(a) (b)

(c)

Figure 4.1. Arsenic test sample (a) before sonication, (b) after sonication, and (c) samples rotating at end-over-end tumbler

Adsorption of Arsenic present in Natural Groundwater

Adsorption of arsenic from groundwater was analyzed in batch adsorption tests similar to those described above. The only difference is in step (iii) where BUET groundwater was used instead of deionized water to prepare a solution with arsenic concentration of 1.0 ppm. It may be noted that the BUET groundwater has arsenic

concentration below 1 μg/L (μDL for AAS used in analysis) no buffer was used to control the pH, and the tests were conducted at natural pH (i.e., pH of the natural ground water). The magnetite nanoparticles concentration was maintained at 0.1 g/L.

Effect of pH on Adsorption of Arsenic

Effect of pH on adsorption of arsenic on MNP was assessed by batch adsorption experiments similar to those described earlier, except no biological buffer was used in step (ii). After filling the glass volumetric flasks to 50 ml mark with deionized water, the pH of the solution was varied by adding diluted standard (0.5 M) hydrochloric acid or sodium hydroxide in amounts of several micro liters. In these adsorption experiments the arsenic concentration was kept constant at 1.0 ppm. The dilute acid and base solutions were used to achieve a wide range of pH (pH = 3~10).

Adsorption of Phosphate

Arrangements of the batch adsorption tests for phosphate were similar to those discussed earlier except that instead of arsenic, standard stock solution of phosphate (10 ppm) was used to prepare the aqueous solution. The initial phosphate concentrations were taken as 0.1 ppm, 0.5 ppm and 1.0 ppm. The pH of the solution was kept constant at 6.1 using 5.0 ml of 0.5 M MES buffer and 0.75 ml of 1.487 M NaOH. The concentration of magnetite nanoparticles was 0.1 g/L. Phosphate concentration was determined using a spectrophotometer (Hach, DR4000U). The difference between the initial and residual phosphate concentration indicated the quantity of adsorbed phosphate on magnetite nanoparticles.

Effect of Phosphate on Arsenic Adsorption

Effect of phosphate concentration on adsorption of arsenic on MNP was evaluated in similar batch experiments described earlier. In these experiments, MNP concentration was 0.1 g/L, arsenic (both arsenate and arsenate) concentration was fixed at 0.5 ppm, while phosphate concentration was varied from 0.10 ppm to 0.50 ppm. The concentration of phosphate was varied by adding required amount of phosphate stock

solution of 10ppm in step (ii). In all experiments, pH was also kept constant at 6.1 (using 5.0 ml of 0.5 M MES buffer and 0.75 ml of 1.487 M NaOH). Residual phosphate concentration was determined using a spectrophotometer (Hach, DR4000U), while arsenic concentration was determined using AAS attached with a graphite furnace (GF-AAS). The difference between the initial and residual phosphate and arsenic concentrations gave the quantity of adsorbed phosphate and arsenic respectively on magnetite nanoparticles.

Kinetics of Arsenic adsorption on Magnetite Nanoparticles

Kinetics of adsorption of arsenic on MNPs was performed in batch experiments. The rate of arsenic adsorption is an important factor for arsenic removal. For this experiment, 5 ml of arsenic (arsenite or arsenate) stock solution of 100 ppm was added in a 500 ml glass volumetric flask, along with 50 ml of 0.5 M MES, 5 ml of 0.1 M $NaNO_3$ and 8.5 ml of 1.487 M NaOH. The volumetric flask was then filled to the 500 ml mark with distilled water. Finally the 500 ml solution was taken in a glass beaker. The initial arsenic concentration of the solution was 1.0 ppm with a background electrolyte concentration of 0.01 M $NaNO_3$. The pH of the solution was fixed at 6.1. The solution was constantly stirred with a magnetic stirrer. Then 0.05 g of MNP was added to the solution (to make the concentration of the MNPs 0.1 g/L) with 10 minutes of sonication for dispersion of the MNPs in the solution. Starting of the reaction time was taken from the time when sonication was stopped. Approximately 10 ml aliquots were taken from the suspension at the following intervals: 0.5, 1.0, 1.5, 2.0, 2.5, 3.0, 3.5, 4.0, 4.5, 5.0, and 22.0, 23.0, 24.0 hours from the start of the reaction time. During this time period, a magnetic stirrer was used to agitate the suspension. The collected samples were taken in a 15ml centrifuge tube and centrifuged for 10 minutes to separate the MNP. The relatively clear and supernatant samples were then filtered through a 0.2 μm Nalgene syringe filter (Surfactant Free Cellulose Acetate, SFCA). Arsenic concentration of the filtrate was measured after suitably diluting the sample. The amount of adsorbed arsenic was estimated by using the initial and final concentrations of arsenic in the aqueous solution.

4.2.2 Laboratory analysis of water samples

Arsenic concentrations were determined with an AAS (Shimadzu, Japan, AA6800) attached with a graphite furnace (GF-AAS). Detection limit of arsenic in this system was 1μg/L Iron concentrations were determined with flame emission atomic absorption spectrophotometer, using an AAS (Shimadzu, Japan, AA6800). Detection limit of iron was 20 μg/L. pH was determined using a pH meter (HACH Co., USA) and phosphate concentration was determined with a spectrophotometer (HACH Co. USA, DR4000U). Phosphate was measured by the Molybdenum Blue method and the detection limit was 0.01 mg/L.

Standard QA/QC procedure was followed throughout including replicate analysis (1 in every 5 samples), checking of method blanks (1 in every 10 analysis) and standards (1 in every 10 analysis).

4.2.3 Chemicals and reagents used

All chemicals used in this study were of analytical grade with deionized water from a Barnstead Fistreem III Glass Still distiller was used. Stock solutions of arsenic (1000±10 mg/L as As^{3+}, prepared from As_2O_3; May & Baker Ltd., Dagenham, England and 1000±10 mg/L as As^{5+}, prepared from $Na_2HAsO_4.7H_2O$; MERCK, E. Merck, Darmstadt) were used for preparation of standard solutions for AAS. Arsenic standard solutions of 10, 20, 25, 30 μg/L were prepared for GF-AAS analysis. Iron standard solutions of 1, 2, 3 and 4 mg/L were prepared for Flame-AAS analysis. Stock solution of phosphate (100±1.0 mg/L as PO_4, HACH Co., USA) was used for preparation of standard solutions for measurement of phosphate concentrations using a spectrophotometer (HACH Co., USA). Magnetite Nanoparticles were procured from Nanostructured and Amorphous Materials, Inc. (16840 Clay Road, Suite 113 Houston, TX 77084, USA). Standard solution were prepared daily throughout the laboratory experimental test time. All acids used in this study were of analytical grade. Hydrochloric acid (fuming 37%, extra pure, Merck, Germany), Nitric acid

(65%, extra pure, Merck Germany) and Sulfuric acid (95-98%, extra pure, Merck, Germany) were used throughout.

4.3 Results and Discussion

4.3.1 Adsorption of arsenic on magnetite nanoparticles

The adsorption characteristic of arsenic was assessed through adsorption isotherms. The adsorption capacities of the magnetite nanoparticles for As(III) and As(V) were evaluated using the isotherms presented in Fig. 4.2 and 4.3, respectively.

The Langmuir and Freundlich equations were employed to describe the adsorption isotherms in the figures. The maximum adsorption calculated from the Langmuir equation was used as the arsenic adsorption capacity. The adsorption constants obtained from the isotherms at different experimental conditions are listed in Table 4.1. As shown in Table 4.1, relatively high regression coefficients (R^2) suggest that both Langmuir and Freundlich models are suitable for describing the adsorption behavior of arsenic by magnetite nanoparticles.

Table 4.1. Langmuir and Freundlich isotherm parameters for As(V) and As(III) adsorption on Magnetite Nanoparticles

		Langmuir Model			**Freundlich Model**		
pH	As species	q_{max} (μmol/g)	b (L/μmol)	R^2	K	n	R^2
5.15	As(III)	550	0.16	0.9990	42.66	0.67	0.9657
6.1		667	0.04	0.9691	25.49	0.76	0.9803
7.5		450	0.08	0.9647	32.06	0.64	0.9671
5.15	As(V)	600	0.13	0.9626	59.84	0.59	0.9428
6.1		500	0.06	0.9934	68.58	0.38	0.9105
9.3		300	0.04	0.9240	10.17	0.80	0.9876

The adsorption data presented in Table 4.1 shows that maximum arsenite, As(III) and arsenate, As(V) adsorption capacity, (q_{max}) on MNPs are 667 μmol/g at pH 6.1 and 600 μmol/g at pH 5.15, respectively. At pH 6.1, arsenite adsorption exceeds the maximum arsenate adsorption on MNPs under the experimental condition employed in the study.

The Langmuir and Freundlich isotherms describe crucial adsorption characteristics of MNPs for arsenic removal. As discussed in Section 2.7.2, the Langmuir isotherm limits the accumulation of adsorbate (As) on adsorbent (MNP) with single layer. After completion of monolayer a flattered isotherm curve gives the idea that no further accumulation on MNPs as it fills all the sites of the adsorbent.

In case of Freundlich isotherm, the pattern of the curve is different from that of Langmuir because it exhibits multilayer adsorption. The free energy of surface sites is reduced by accumulation of As on MNPs. Thus, the isotherm curves show gradual increase due to adsorption of arsenic with increased aqueous concentrations and it enumerates exponential decrease in free surface energy sites therefore exponential increase in particle adsorption. High regression coefficients (R^2>0.97) suggested that both Langmuir and Freundlich models were suitable for describing the adsorption behavior of As(III) and As(V) by magnetite nanoparticles.

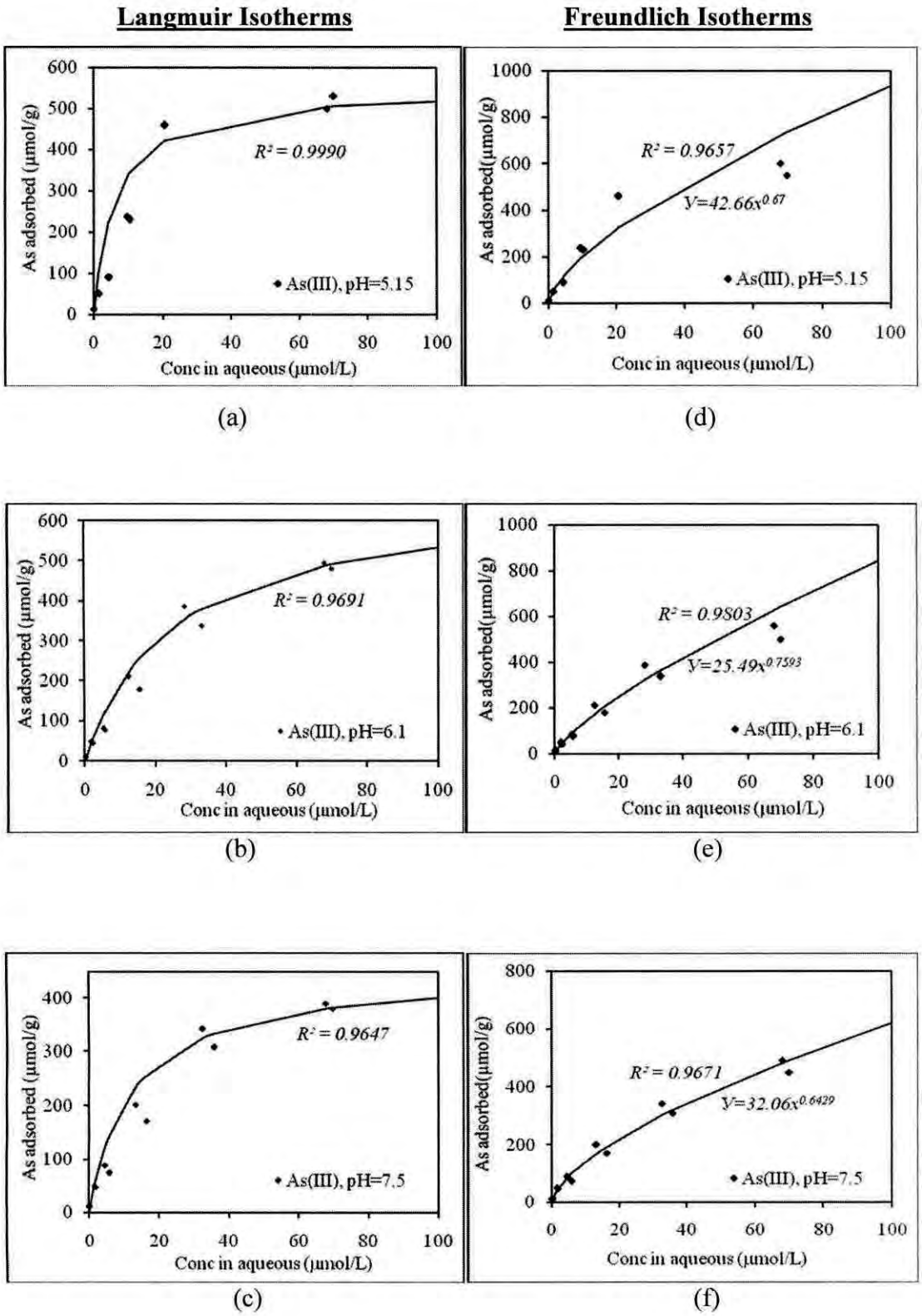

Figure 4.2. Adsorption of arsenite on magnetite nanoparticle of concentration 0.1 g/L at pH values 5.15, 6.1, and 7.5

Langmuir Isotherms **Freundlich Isotherms**

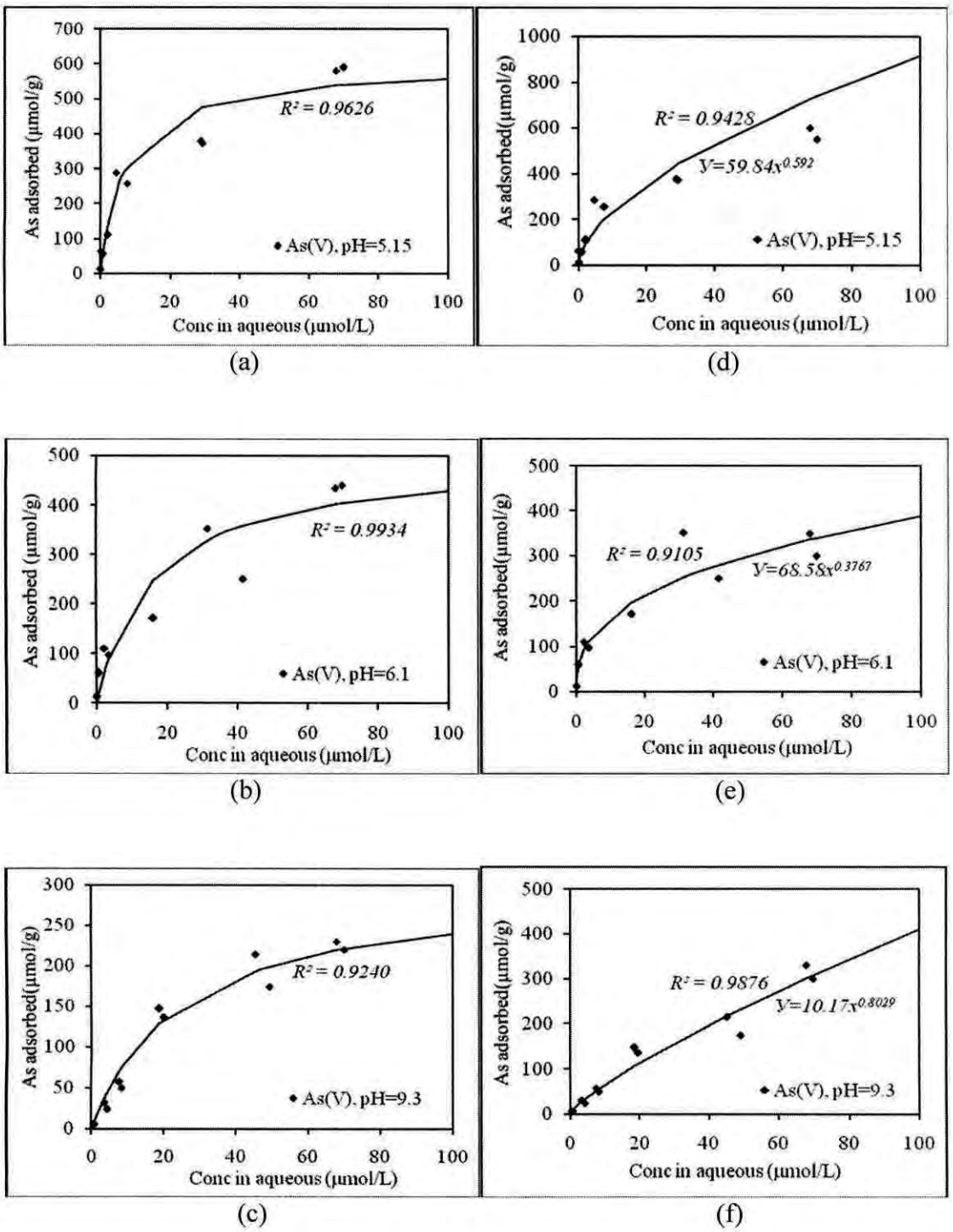

Figure 4.3. Adsorption of arsenate on magnetite nanoparticle of concentration 0.1 g/L at pH values 5.15, 6.1, and 9.3

The q_{max} values obtained for the magnetite nanoparticles are compared with those obtained using other adsorbents in Table 4.2.

Table 4.2. Maximum arsenic adsorption capacities of some adsorbent systems

Adsorbent	**Max. As(III)**	**Max. As(V)**	**Reference**
	Adsorption capacity ($mmolg^{-1}$)	**Adsorption capacity ($mmolg^{-1}$)**	
Magnetite Nanoparticles	**0.67 (pH 6.1)**	**0.60 (pH 5.15)**	**Present study**
MnO_2	0.13	0.1	Lenoble *et al.* (2004)
Geothite	/	0.53 (pH 3-3.3)	Matis *et al.* (1997)
$Al_2O_3/Fe(OH)_3$	0.12 (pH 6.1)	0.49 (pH 7.2)	Hlavay and Polyák (2005)
Fe(III)-loaded sponge	0.24 (pH 6.1)	1.83 (pH 4.5)	Muñoz *et al.* (2002)
Fe-Mn-mineral material	0.16 (pH 6.1)	0.09 (pH 5.5)	Deschamps *et al.* (2005)
TiO_2	0.43 (pH 6.1)	0.55 (pH 7.0)	Bang *et al.* (2005)
Hematite Nanoparticles	0.59 (pH 6.1)	0.30 (pH 6.1)	Choudhury (2009)

Most of the traditional media used for arsenic removal has very low selectivity for arsenite. It should be noted that majority of arsenic in natural groundwater exists as arsenite (WHO, 2005). The increased maximum adsorption capacity for arsenite in this study suggests that magnetite could be a potential adsorbent for arsenite removal from water. Therefore, it appears that magnetite nanoparticle could be very appropriate for both arsenite and arsenate removal from water.

Previous works regarding adsorption of arsenic on magnetite nanoparticles (Yean *et al.*, 2005) showed that arsenic adsorption isotherm appeared to consist of two Langmuir type isotherms for both arsenite and arsenate. Figure 4.4 shows the adsorption isotherms for As(III) and As(V) on magnetite nanoparticles (size: 11.72

nm) reported by Yean *et al.*, (2005). It shows that at low concentration, the adsorption isotherms can be fitted with a simple Langmuir Isotherm. However, at high As concentrations, the adsorption data deviates from the simple Langmuir isotherm, and appears to follow a second Langmuir isotherm.

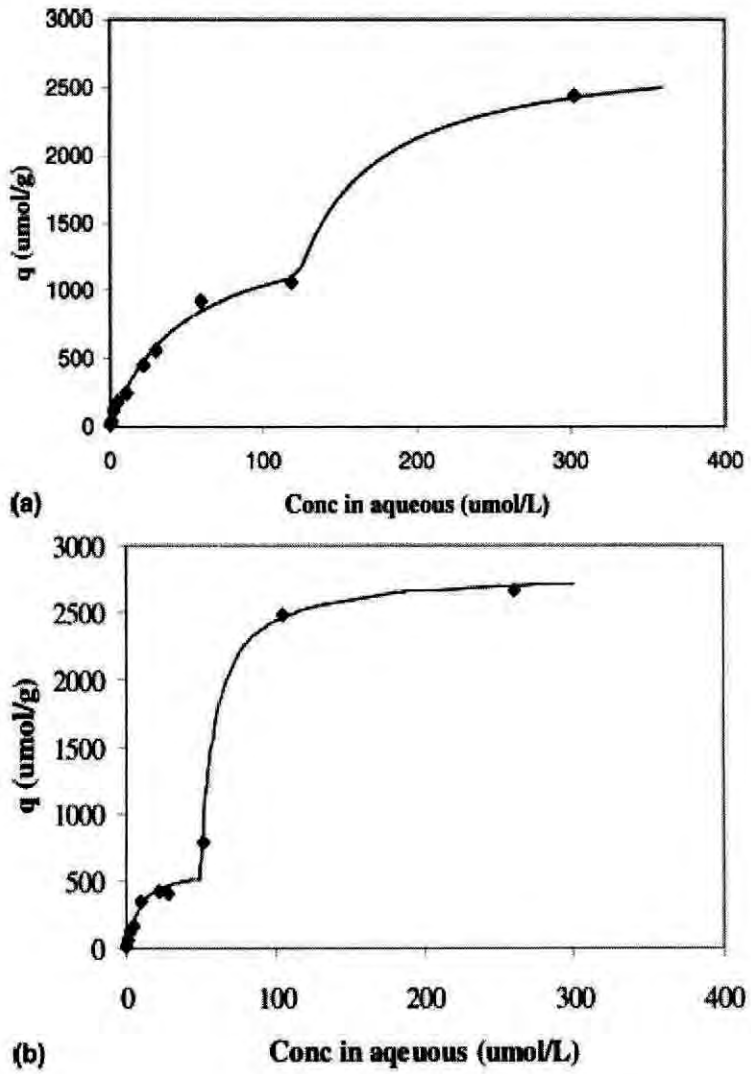

Figure 4.4. Adsorption of Arsenic to 11.72 nm magnetite at pH 8.0:
(a) As(III) and (b) As(V) (Yean *et al.*, 2005)

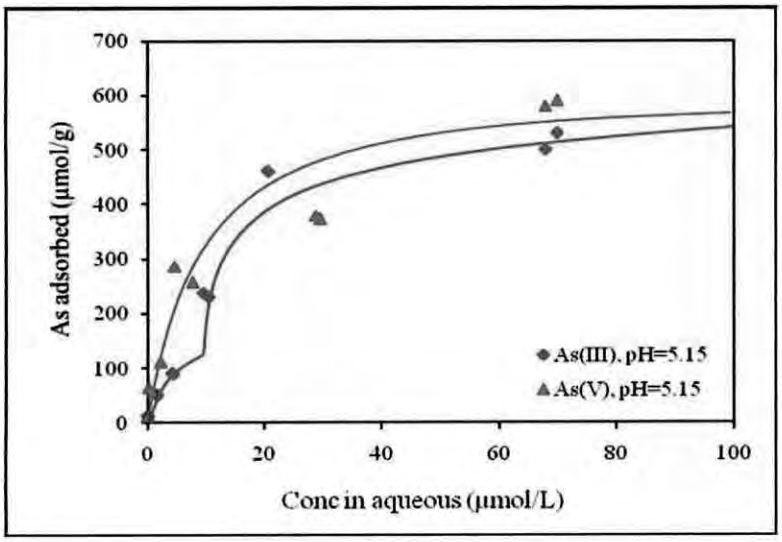

(a)

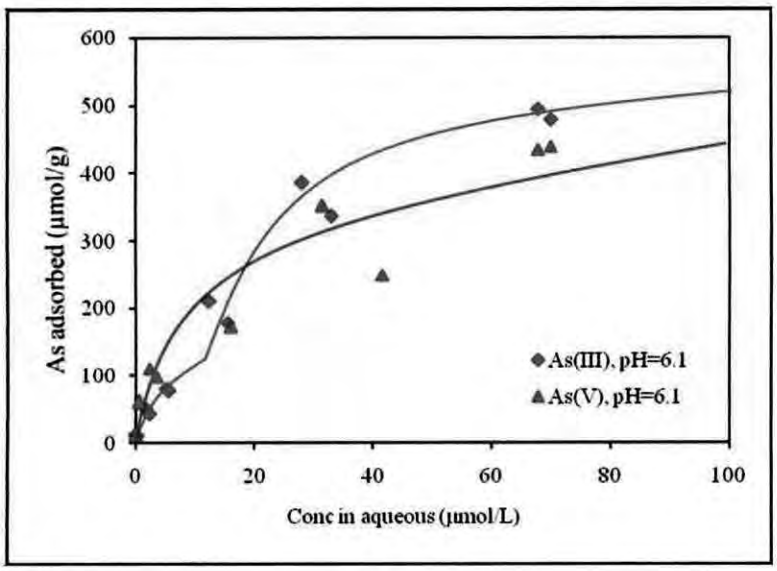

(b)

Figure 4.5. Adsorption of arsenite and arsenate on MNPs at pH (a) 5.15, and (b) 6.10

The reason behind the discussion above is that if we pay a closer look at the Langmuir isotherm curves at pH 5.15 and 6.1 for arsenite (see Fig. 4.5), we see a similar pattern of curve with that of Figure 4.4. Figure 4.5 shows two Langmuir type adsorption isotherms for arsenite at relatively low and high aqueous concentrations at a particular pH.

At pH value 5.15, though there are two Langmuir adsorption isotherms for arsenite, it does not overshoot the arsenate isotherm. At low concentration [<15 μmol/L], the adsorption isotherm can be fitted with simple Langmuir isotherm. But beyond that concentration, a second Langmuir isotherm could be fitted to describe the data. Again at pH 6.10 a second Langmuir adsorption isotherm could be fitted to describe arsenic adsorption at higher concentration [>17 μmol/L].

Adsorption of arsenite on MNPs does have a major change between pH values of 5.15 and 6.10. The adsorption of arsenite on MNPs exceeds that of arsenate at pH 6.10 at higher concentration [>20μmol/L], whereas it does not exceed arsenate adsorption at pH 5.15. This reveals a higher arsenic adsorption capacity of MNP at pH 6.10 compared to 5.15.

4.3.2 Effect of pH on arsenic adsorption

Figure 4.6 shows effect of pH on adsorption of both arsenite and arsenate on MNP. The figure shows that at low pH range both arsenite and arsenate are removed more rather than those at high pH values. As can be seen, the As(V) removal was evidently dependent on pH with the greatest adsorption occurring under acidic conditions and decreased with increase in solution pH. $H_2AsO_4^-$ and $HAsO_4^{2-}$ are dominant As(V) species in the solution under the experimental conditions (pH range 3~10). Lower pH is favorable for the protonation of sorbent surface. Increased protonation is thought to increase the positively charged sites, increase the electrostatic attraction force existing between the sorbent surface and arsenic anions and therefore increase the amount of adsorption in the lower pH region. But in higher pH region, the negatively charged sites dominate, the electrostatic repulsion effect enhances, and the amount of adsorption is consequently reduced.

The same trend is also observed with the As(III), but the decrease in As(III) removal was not as significant as that of As(V) with increasing pH. Many studies also suggest that increasing pH decreased As(V) adsorption on iron or iron containing adsorbents (Jang *et al.*, 2006), which is typical of anionic adsorption. These studies also indicate

that the effect of pH on As(III) adsorption on iron adsorbents is very different from that of As(V), since H_3AsO_3 is the dominant dissolved As(III) species at pH below 9.2. For the present adsorbent (MNP) in this study, no significant decrease in As(III) removal was observed until the solution pH was increased to 5.5, indicating that the material will have lower arsenic adsorption for majority of water samples, which normally have a pH range of 6.5-8.5 (Gu *et al.*, 2005).

Aggregation could have a significant influence on arsenic adsorption on MNPs. In the pH range from 3.0 to 7.0 the surface charge of the magnetite nanoparticle is positive as pH_{pzc} = 7.0 (Section 3.3.4). As(V) was adsorbed more than As(III) on MNPs at pH <6.0. But at pH value>6.0, As(III) was adsorbed more than As(V). With increasing pH the surface charge changes gradually to zero at pH = 6.0~7.0. After that the surface charge becomes negative at higher pH values (>7.0) and negative As(V) species have electrostatic repulsive behavior with MNPs surface sites and hence less As(V) was adsorbed than As(III) on MNPs. On the other hand, As(III) remains undissociated (H_3AsO_3) at pH<9.2, therefore, charged particle surface sites have little effect on its adsorption on MNPs. The pH effect on aggregation is mainly due to the fact that pH affects particle surface charge.

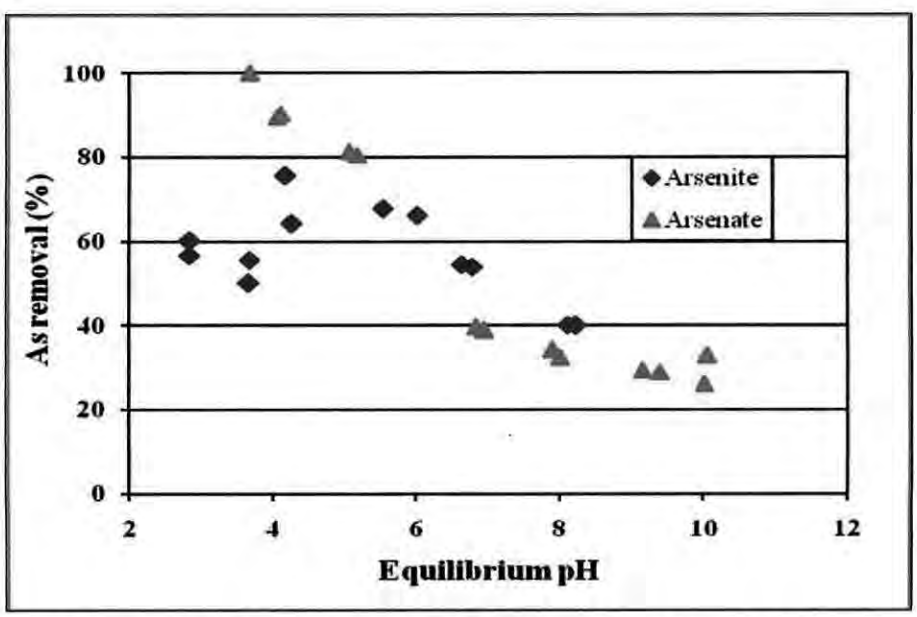

Figure 4.6. Effect of pH on adsorption of As(III) and As (V) with MNP at 0.1 M ionic strength. (0.133 mol As / kg Magnetite)

Adsorption of arsenic from groundwater

The adsorption of arsenic from BUET groundwater was evaluated at natural pH (pH = 7.7) of the groundwater, with a magnetite nanoparticles concentration of 0.1 g/L. The groundwater was collected from a deep tube-well near the Administrative Building of BUET and results of adsorption of arsenic on nanoparticles are shown in Table 4.3. Table 4.3 shows that adsorption of both As(III) and As(V) are comparable. The amount of As adsorbed, presented in Table 4.3, are less than those achieved during laboratory batch experiments (under similar conditions), which were conducted using only aqueous solutions of arsenic.

Table 4.3. Adsorption of Arsenic from Groundwater on Magnetite Nanoparticles (0.1 g/L) at pH 7.7. (Initial Arsenic Concentration = 1.0 ppm)

Arsenic Species	Residual Arsenic Concentration ($mmolg^{-1}$)	Adsorbed Arsenic ($mmolg^{-1}$)	Percentage of Arsenic adsorbed
As(III)	5.41	4.59	45.9
As(V)	6.88	3.12	31.2

Previous research (Sharma, 2006 and Zhang *et al.*, 2007) has shown that arsenic sorption to mineral surfaces decreases in the presence of competing anions such as phosphate, silicate, sulfate, nitrate, carbonate as well as natural organic matter (NOM). Hence the presence of such competing anions in the groundwater may be responsible for the observed lower adsorption of arsenic from natural groundwater. Also at the pH value of 7.7 at which these experiments were carried out, the surface of the MNPs was negative. The presence of cations like Ca^{2+}, Mg^{2+} those promote double layer compression resulting less arsenic adsorption on MNPs.

4.3.3 Adsorption of phosphate on MNP

Table 4.4. Adsorption results of Phosphate on Magnetite Nanoparticles			
Initial Phosphate Concentration. (ppm)	Residual Phosphate Concentration (ppm)	Adsorbed Phosphate. (ppm)	% of Phosphate Adsorbed
0.1	0.044	0.056	56
0.5	0.198	0.302	60.4
1.0	0.566	0.434	43.4

Adsorption of phosphate on MNPs is shown in the Table 4.4. The adsorption experiments were conducted at pH 6.10 with only deionined water. The concentration of MNPs was 0.1 g/L. We find that adsorption of phoshate decreases with increased phosphate concentrations.These results suggest that phosphate could effectively compete with arsenic for adsorption onto MNPs.

4.3.4 Effect of phosphate on arsenic adsorption

Among the anions which could compete effectively with arsenic for adsorption site on a sorbent, Phosphate is ubiquitous in natural groundwater. Groundwater in Bangladesh also contains high concentrations of phosphate (0.2-3.0 mg/L) (Meng *et al.*, 2000). So its potential influences on arsenic sorption and mobility are significant. Phosphate sorbs strongly onto iron oxide minerals and can therefore compete with arsenic for surface sites (Dixit and Hering, 2003). Figure 4.7 shows adsorption of arsenic on MNP at fixed pH of 6.10 ± 0.05, in the presence of 3 (three) different PO_4^{3-} concentrations (0.1, 0.25 and 0.5 ppm). The concentration of arsenic in suspension was 0.5 ppm.

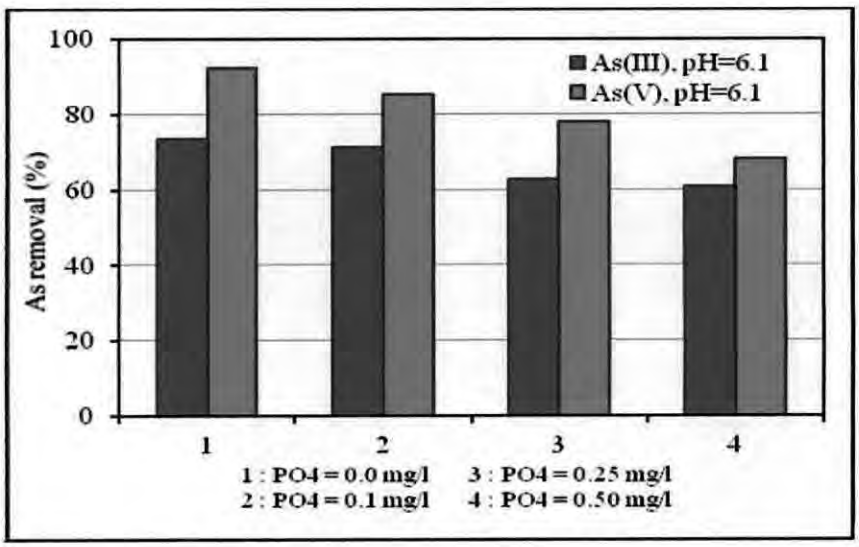

Figure 4.7. Effect of phosphate (competing anion) on arsenic removal with arsenic concentration of 0.5 ppm at pH 6.10 with 0, 0.1, 0.25, and 0.5 ppm Phosphate

Figure 4.7 clearly shows the effect of phosphate on adsorption of arsenic as a competing anion. The results show about 13% decrease in adorption of arsenite in the presence of 0.50 ppm phosphate whereas the corresponding figure for arsenate is about 25%. Phosphate and arsenic lie in same group in the Periodic Table (Gr VA), but the atomic number of phospahte (15) is less than that of arsenic (33). Therefore, phosphate competes well for adsorption onto different adsorbents and this study provides evidence for this characteristics.

4.3.5 Kinetics of aresnic adsorption on MNPs

Kinetics of adsorption gives the idea of rate of arsenic adsorption on MNPs. It provides time behavior of arsenic removal by MNPs.In the kinetic experiment, the aqueous arsenic concentration was 13.3 μM, with 0.1 g/L concentration of adsorbent and solution pH was kept at 6.10.

Figure 4.8 shows adsorption of arsenic as a function of time from the kinetic experiment. From the fugure it is seen that adsorption of arsenate is relatively faster

than arsenite. After 24 hour, the final ramoval for arsenate was about 79% whereas this value is 62% for arsenite. Most of the adsorption for arsenate was complete within 2 hours from the start of experiment. But in case of arsenite, the adsorption continued for upto 5 hours. The last 3 data in each experiment were almost same, which indicates that the adsorption reached equilibrium within 24 hour. Then results validate the 24 hour equilibration period used in the adsorption experiment.

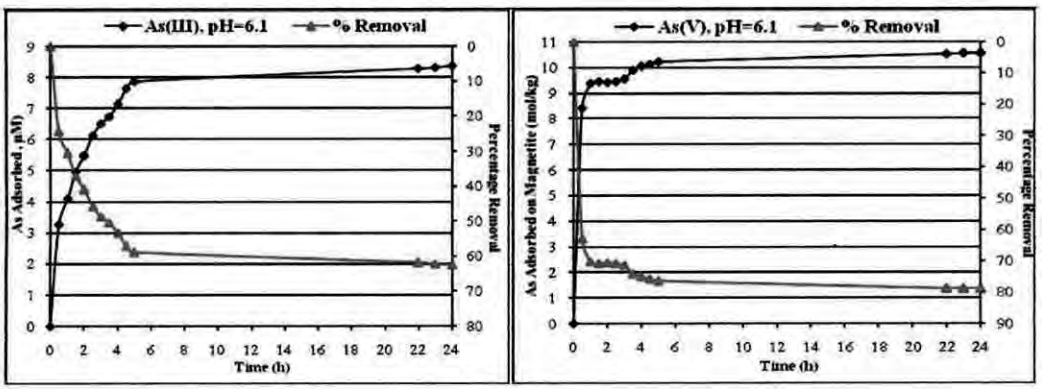

(a) (b)

Figure 4.8. Adsorption kinetics on magnetite nanoparticles of (a) As(III), and (b) As(V) at pH 6.10. Initial arsenic = 13.3 µM, and adsorbent = 0.1 g/L

Kinetic rate constants for the pseudo first order kinetic model and pseudo second order kinetic model were determined from the following two equations (described in article 2.8):

$$\log(q_e - q) = \log q_e - \frac{k_1 t}{2.303} \quad \text{..... (First-order kinetic model)}$$

$$\frac{t}{q} = \frac{1}{k_2 q_e^{\,2}} + \frac{t}{q_e} \quad \text{..... (Second-order kinetic model)}$$

Figures 4.9 and 4.10 show the plots of $\log(q_e - q)$ *versus* t and t/q *versus* t, respectively, from which the kinetic rate constants were determined. Table 4.6 lists the computed

results obtained from the first-order and the second-order kinetic model and also the experimentally observed values of q_e.

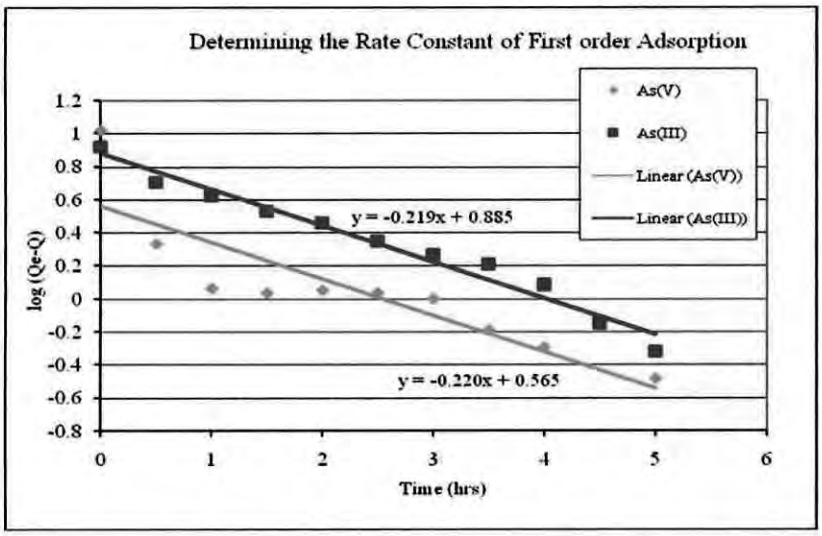

Figure 4.9. $\log(q_e - q)$ *versus t.* (Slopes and Intercepts of the graphs were used to determined Reaction Rate Constant k_1, and amount of arsenic adsorbed in equilibrium q_e)

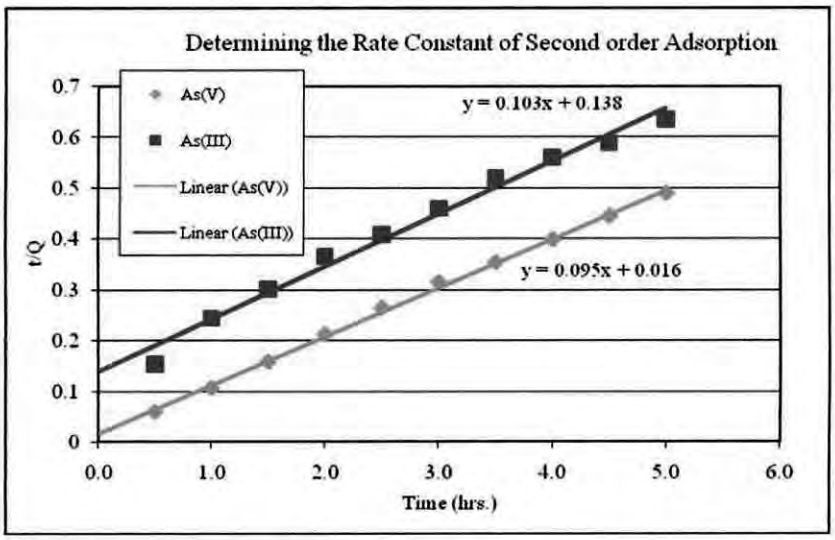

Figure 4.10. *t/q versus t.* (Slopes and Intercepts of the graphs were used to determined Reaction Rate Constant k_2, and amount of arsenic adsorbed in equilibrium q_e)

Table 4.5. The first-order and second-order adsorption rate constants and calculated q_e values for both As(V) and As(III) on MNPs				
Arsenic	First-order kinetic model (from figure 4.9)		Second-order kinetic model (from figure 4.10)	
	k_1 (hr^{-1})	$q_{e,cal}$ (μM)	k_2 ($\mu M^{-1}hr^{-1}$)	$q_{e,cal}$ (μM)
As (V)	0.507	3.6728	0.564	10.5263
As (III)	0.504	7.6736	0.077	9.7087

Table 4.5 gives values of adsorption rate constants (k) and calculated adsorption of As at equilibrium, q_e for first-order and second-order kinetic models found from Figure 4.9 and 4.10.

Table 4.6. Comparison of experimental and predicted adsorption (using first-order and second-order kinetic models) of As(III) and A(V) on MNPs (Initial As concentration = 13.3 μM)				
Arsenic species	Time, t (hr)	First-order kinetic model	Second-order kinetic model	Experimental values of adsorption of As on MNPs (μM)
		Amount of As adsorbed (μM) on MNPs	Amount of As adsorbed (μM) on MNPs	
As (V)	0	0	0	0
	2	2.3393	9.7088	9.4087
	5	3.3811	10.183	10.2077
	24	3.6728	10.453	10.5366
As (III)	0	0	0	0
	2	4.8746	5.8177	5.4693
	5	7.057	7.659	7.8728
	24	7.6736	9.1961	8.3549

Table 4.6 shows comparison of adsorption of As on MNPs for first-order and second-order kinetic models with those found from experiments. It is found that only As(V) adsorption satisfies first-order kinetic model but both the models quite satisfy As(III) adsorption on MNPs.

4.4 Summary

Adsorption of arsenic on MNPs was assessed. Adsorption of arsenic on MNPs was described by Langmuir and Freundlich Isotherms. Both the isotherms were described the experimental data quite well at different pH and solution concentrations. The maximum adsorption of arsenite and arsenate on MNPs were found to be 667 μmol/g at pH 6.10 and 600 μmol/g at pH 5.15, respectively in aqueous solution containing 0.01 M $NaNO_3$. At pH 5.15, a second Langmuir adsorption isotherm was observed for arsenite. At low arsenic concentration (<15 μmol/L), the adsorption isotherm can be fitted with simple Langmuir isotherm. Same case happened at pH 6.10 for arsenite where second Langmuir isotherm appeared after 17 μmol/L aqueous concentration.

The pH of the aqueous solution has a strong influence on arsenic adsorption on MNPs. The effect of pH for arsenite and arsenate is not same in pH ranging from 3 to 10. Adsorption of arsenate on MNPs was higher at pH below 6.0 and relatively lower at pH values >6.0. On the other hand there was no significant effect of pH on arsenite adsorption on MNPs. At high pH (>7.0) arsenite adsorption was higher than arsenate adsorption on MNPs.

Adsorption of arsenic present in natural groundwater was also assessed. It was found that arsenic adsorption was relatively less compared to those in deionized water (with 0.01 M $NaNO_3$). Presence of competing anions such as PO_4^{3-}, silicate, sulfate, nitrate, carbonate etc. and aggregation of MNPs are probably responsible for lower adsorption of arsenic.

Similar to the effect of pH, the effect of phosphate on arsenic adsorption on MNPs was evaluated. The adsorption of arsenite and arsenate (present with an initial

concentration of 0.5 ppm) on MNPs reduced by about 13% and 25%, respectively in presence of 0.5 ppm phosphate in solution.

The adsorption of arsenate was found to be faster than that of arsenite on MNPs. Kinetic adsorption data were fitted by first and second order kinetic models and it was found that the rate of arsenate adsorption did not satisfy first order kinetic model whereas both the models described arsenite and arsenate adsorption on MNPs very well.

Chapter 5

CONCLUSIONS AND RECOMMENDATIONS

5.1 Conclusions

The present research work commenced with an aim to achieve the following objectives: (1) Characterization of commercially procured magnetite nanoparticles, (2) Assessment of arsenic adsorption characteristics of magnetite nanoparticles, which included the effect of different water quality parameters like pH, phosphate content along with evaluation of adsorption kinetics.

These objectives were set to understand the adsorption mechanism of arsenic on magnetite nanoparticles under different conditions. The major conclusions from this study are summarized below:

i. The physical qualities of the magnetite nanoparticles mentioned by the manufacturer were different from that observed in the characterization test results. This finding points out to the essential requirement of characterizing the procured nanomaterials from the vendors. It was seen that the reported specific surface area of the nanoparticles (60 m^2/g) was very high compared to the specific surface area 37.7 m^2/g determined in this study. The internal pore size range of MNPs is about 15-28 °A. The structure, composition and particle size of the magnetite nanoparticles agreed to the mentioned features. The hydrodynamic radius (R_h) of MNPs was measured as 193.1±5.7 nm which is over eight times the original particle size. The pH of zero surface charge (pH_{pzc}) of MNPs was 7.0.

ii. The adsorption isotherm developed from the experimental results shows that both Langmuir and Freundlich isotherms represent the adsorption data well under different parameters. In Langmuir isotherm, the maximum adsorption of arsenite on MNPs is 667 μmol/g at pH 6.10 and it is 600 μmol/g at pH 5.15, in case of arsenate. The data of arsenite revealed two Langmuir isotherms at low and high

aqueous concentrations. Second Langmuir isotherm appeared at higher arsenite concentration for pH values 5.15 and 6.10.

iii. Adsorption of arsenic on magnetite nanoparticles depends on different water quality parameters like pH, phosphate content. It was observed that with increasing pH the adsorption of both As(III) and As(V) decreases. Adsorption of As(V) at low pH (<6.0) is higher than that of As(III) whereas at higher pH, adsorption of As(III) is higher than As(V).

iv. The adsorption of arsenic on MNPs decreased when conducted with natural groundwater compared to adsorption in de-ionized water with an electrolyte.

v. The adsorption of arsenic [both As(III) and As(V)] is decreased in the presence of phosphate ion. Hence presence of phosphate in water reduces the efficiency of magnetite nanoparticles as adsorbents for arsenic.

vi. Magnetite nanoparticles adsorb to their maximum capacity in almost 5 hours of contact time with the solution.

107242

5.2 Recommendations

The following are recommended for future studies:

1) The desorption characteristics of magnetite nanoparticles should be analyzed in order to find the desorption hysteresis at different pH. This will lead to the evaluation of possible regeneration capacity of the magnetite nanoparticles to be used in a filter media for practical application.

2) Studies should be carried out to find the possibility of dispersing the magnetite nanoparticles into a porous or solid polymeric matrix which will retain the nanoparticles in place and allow them to come in contact with water flowing through the porous material. This way the arsenic present in the water will be adsorbed by the nanomaterials and the entire system can act as an effective filter media.

3) Field study should be carried out to see the effect of direct subsurface injection of magnetite nanoparticles, whether under gravity-fed or nanoparticle-water slurry, in areas with high arsenic concentration in groundwater of Bangladesh. It will enable assessment of the potential application of the magnetite nanoparticles for immobilization of heavy metals like arsenic.

4) Efforts should be made to use surface complexation models (SCMs) for describing the experimental data.

REFERENCES

Ahmed. F. , Jalil, M.A., Ali, M.A., Hossain, M.D., and Badruzzaman, A.B.M. (2000): An overview of arsenic removal technologies in BUET, In *Bangladesh Environment-2000*, M.F.Ahmed (Ed.), Bangladesh Poribesh Andolon, 177-188.

Badruzzaman, M., and Westerhoff, P. (2005): "Field and lab-based evaluation of packed bed arsenic treatment systems", AWWA Annual Conference and Exhibition, San Francisco, CA.

BAMWSP, DFID and WaterAid Bangladesh (2001): *Rapid Assessment of Household Level Arsenic Removal Technologies*, Phase-I and Phase-II, Final Report, WS Atkins International Limited.

BAMWSP (2005): Bangladesh Arsenic Water Supply Project, Website: www.bamwsp.org.

Bang, S., Patel, M., Lippicott, L., and Meng, X.G. (2005): Removal of arsenic from groundwater by granular titanium dioxide adsorbent. Chemosphere 60 (3), 389–397.

Barrett, E. P., Joyner, L. G., and Halenda, P. P. (1951): "The Determination of Pore Volume and Area Distributions in Porous Substances. I. Computations from Nitrogen Isotherms", *J. Am. Chem. Soc.* 1951, 73, 373-380.

Berdal, A., Verrié, D., and Zaganiaris, E. (2000): "Removal of arsenic from potable water by ion exchange resins", In Greig J.A., Ed., Ion Exchange at the illennium. London: Imperial College Press, p. 101.

BGS/DPHE (2001): Arsenic Contamination of Groundwater in Bangladesh, Department of Public Health Engineering , DFID, British Geological Survey.

Bissen, M. and Frimmel, F.H. (2003): Arsenic—A review. Part I: Occurrence, toxicity, speciation, mobility. *Acta Hydroch. Hydrob.* 31, 9.

Brunauer, S., Emmett, P. H., and Teller, E. (1938): "Adsorption of Gases in Multimolecular Layers", *J. Am. Chem. Soc.* 1938, 60, 309-319.

Bulletin of the World Health Organization (WHO) (2005): "Arsenic contamination of groundwater and its health impact on residents in a village in West Bengal, India"

Chen, K. L. and Elimelech, M. (2006): "Aggregation and deposition kinetics of fullerene (C-60) nanoparticles", Langmuir 2006, 22, 10994-11001.

Chen, K. L. and Elimelech, M. (2007): "Influence of humic acid on the aggregation kinetics of fullerene (C-60) nanoparticles in monovalent and divalent electrolyte solutions", *J. Colloid Interf. Sci.* 2007, 309, 126-134.

Chen, K. L., Mylon, S. E., and Elimelech, M. (2006): "Aggregation kinetics of alginate-coated hematite nanoparticles in monovalent and divalent electrolytes." *Environ. Sci. Technol.* 2006, 40, 1516-1523.

Cherry, J.A. (1979): Arsenic species as an indicator of redox conditions in ground water, J. Hydrology vol. 23, page 379-392.

Choudhury, M. R. (2009): Assessment of hematite nanoparticles as adsorbent for arsenic removal – A thesis submitted to the Department of Civil Engineering of Bangladesh University of Engineering and Technology, Dhaka, in partial fulfilment of the requirements for the degree of Master of Science in Civil Engineering (Environmental).

Clarifications to compliance and new source contaminants monitoring (2005): Assessed on April 2005: http://www.epa.gov/safewater/ars/arsenic_finalrule.pdf.

Clifford, D. (2003): An overview of arsenic treatment methods: http://sandia.gov/water/arsenic2003/forumdocs/nmehc_As_treatment.pdf

Dahi, E. (1997): Arsenic and Dearsenization of Water, paper presented in the ITN-B course on Water Supply and Waste Management, during 9th – 12th Aug., ITN Center, BUET, Dhaka.

Deschamps, E., Ciminelli, V.S.T., Holl, W.H. (2005): Removal of As(III) and As(V) from water using a natural Fe and Mn enriched sample. Water Res. 39 (20), 5212–5220.

Dixit, S. and Hering, J.G. (2003): "Comparison of arsenic (V) and arsenic (III) sorption onto iron oxide minerals: Implications for arsenic mobility", *Environ. Sci. Technol.* 37, 4128 (2003).

Driehaus, W., Jekel, M., and Hildebrandt, U. (1998): "Granular ferric hydroxide—A new adsorbent for the removal of arsenic from natural water", *J. Water Serv. Res. Technol.- Aqua*, 47(1), 30.

Freundlich, H. (1926): *Colloid and Capillary Chemistry,* London: Hasseler, J.W. 1974. *Activated carbon,* New York: Chemical Pub. Co.

Groen, J. C., Peffer, L. A. A., and Perez-Ramirez, J. (2003): Pore size determination in modified micro- and mesoporous materials. Pitfalls and limitations in gas adsorption data analysis – Microporous and Mesoporous Materials, 60, 1–17.

Gu, Z., Fang, J. and Deng, B.L. (2005): Preparation and evaluation of GAC-based iron-containing adsorbents for arsenic removal. Environ. Sci. Technol. 39, 3833–3843.

Hlavay, J. and Polya´ k, (2005): Determination of surface properties of iron hydroxide-coated alumina adsorbent prepared for removal of arsenic from drinking water. J. Colloid Interf. Sci. 284, 71–77.

Holm, T. R. (2002): "Effects of carbonate/bicarbonate, silica, and phosphate on arsenic sorption to hydrous ferric oxide." J. Am. Water Works Assoc. **94**(4): 174-181.

Jang, M., Min, S.H., Kim, T.H., and Park, J.K. (2006): Removal of arsenite and arsenate using hydrous ferric oxide incorporated into naturally occurring porous diatomite. Environ. Sci. Technol., 40, 1636–1643.

King, R. J. (2002): "Minerals explained 35: Arsenopyrite". *Geology Today* 18 (2): 72–75. doi:10.1046/j.1365-2451.2002.t01-1-00006.

Lagergren, S. (1898): "Handlinggar", 24, 1.

Langmuir, I. (1918): The adsorption of gases on plane surfaces of glass, mica and platinum, J. Am. Chem. Soc. 40, pp. 1362–1403.

Lenoble, V., Laclautre, C., Serpaud, B., Deluchat, V., and Bollinger, J.C. (2004): As(V) retention and As(III) simultaneous oxidation and removal on a MnO_2-loaded polystyrene resin. Sci. Total Environ. 326, 197–207.

Marmier, N., Delisee, A., and Fromage, F. (1999): Surface complexation modeling of Yb(III), Ni(II), and Cs(I) sorption on magnetite. *J. Colloid Interface Sci.* **211,** 54.

Matis, K.A., Zouboulis, A.I., Malamas, F.B., Ramos Afonso, M.D., and Hudson, M., (1997): Flotation removal of As(V) onto goethite. Environ. Pollut. 97 (3), 239–245.

Mayo, J. T., Yavuz, C., Yean, S., Cong, L., Shipley, H, Yu, W., Falkner, J., Kan, A., Tomson, M., and Colvin, V., L. (2007): The effect of nanocrystalline magnetite size on arsenic removal, *Sci.Technol. Advanced Materials*, 8, 71-75.

Mckay, G. and Ho, Y. S. (1999): "Process Biochem.", 34, 451.

Meng, X., Bang, S., and Korfiatis, G.P. (2000): "Effects of silicate, sulfate and carbonate on arsenic removal by ferric chloride", *Water Res.* 34, 1255.

Mittal, S. K. and Singh, P. (2002): Exchange kinetic studies on Zirconium Antimonophosphate, Indian Journal of Chemistry, 41A, 500-505.

Mun˜oz, J.A., Gonzalo, A., and Valiente, M. (2002): Arsenic adsorption by Fe(III)—loaded opencelled cellulose sponge. Thermodynamic and selectivity aspects. Environ. Sci. Technol. 36, 3405–3411.

Mylon, S. E., Chen, K. L., and Elimelech, M. (2004): Influence of Natural Organic Matter and Ionic Composition on the Kinetics and Structure of Hematite Colloid Aggregation: Implications to Iron Depletion in Estuaries, *Langmuir,* 20, 9000–9006.

North, K.P. (2005): "Attrition loss analysis for arsenic adsorption media", Sandia National Laboratory Report SAND2006-0374.

Plant, J.A., D.G. Kinniburgh, P.L. Smedley, F.M. Fordyce, and B.A. Klinck. (2004): Arsenic and Selenium, p. 17-66, *In* B. S. Lollar, ed. Environmental Geochemistry, Vol. 9. Elsevier Science.

Rubel, F. (2003a): "Removal of arsenic from drinking water by adsorptive media." USEPA Report EPA/600/R-03/019.

Rubel, F. (2003b): "Removal of arsenic from drinking water by ion exchange." USEPA Report EPA/600/R-03/080.

Saleh, N. B., Pfefferle, L. D., and Elimelech, M. (2008): "Aggregation Kinetics of Multiwalled Carbon Nanotubes in Aquatic Systems: Measurements and Environmental Implications", *Environ. Sci. Technol.* 2008, 42, 7963-7969.

Sengupta, A.K. and Cumbal, L.H. (2005): Method of manufacture and use of hybrid anion exchanger for selective removal of contaminating ligands from fluids. US Patent Application No. US 2005/0156136 A1.

Sharma, P., Kumari, P., Srivastava, S., and Srivastava, M.M. (2006): "Biosorption studies on shelled Moringa oleifera Lamarch seed powder: Removal and recovery of arsenic from aqueous system", *Int. J. Miner. Process,* 78: 131-139.

Sing, K. S. W., Everett, D. H., Haul, R. A. W., Moscou, L., Pierotti, R. A., Rouquerol, J., and Siemieniewska, T. (1985): "Reporting Physisorption Data for Gas/Solid Systems with Special Reference to the Determination of Surface Area and Porosity", *Pure & Appl. Chem.*, Vol. 57, No. 4, pp. 603—619, 1985. Printed in Great Britain. ©1985 IUPAC.

Smedley, P.L. and Kinniburgh, D.G. (2002): A review of the source, behavior and distribution of arsenic in natural waters. Appl. Geochem. 17, 517–568.

Stumm, W. and Morgan, J.J. (1995): *Aquatic Chemistry: Chemical Equilibria and Rates in Natural Waters* (Wiley-Interscience, New York, 1995).

Subramanian, K. S., Thirunavukkarasu, O. S., and Viraraghavan, T. (2004): Arsenic Removal from Drinking Water using Iron Oxide-Coated Sand, journal of water air and soil pulltion, earth and environmenta sci. volume 142, 95-111.

Sylvester, P., Westerhoff, P., Boyd, O., and Sengupta, A.K. (2005): ArsenX*np*-A new hybrid sorbent for arsenic removal from drinking water. ACE '05, *Proceedings of the AWWA Annual Conference and Exposition,* San Francisco.

Sylvester, P., Westerhoff, P., Möller, T., Badruzzaman, M., and Boyd, O. (2007): "A Hybrid Sorbent Utilizing Nanoparticles of Hydrous Iron Oxide for Arsenic Removal from Drinking Water", *ENVIRONMENTAL ENGINEERING SCIENCE*, Volume 24, Number 1, 2007, © Mary Ann Liebert, Inc.

Tewari, P.H. and McClean, A.W. (1972): Temperature dependence of point of zero charge of alumina and magnetite. *J. Colloid Interface Sci.* **40,** 267.

Yamamura, S. (2003): Drinking water guidelines and standards. In Arsenic, Water, and Health: the state of the art (eds. H. Hashizume and S. Yamamura). World Health Organisation, chap. 5.

Yean, S., Cong, L., Yavuz, C.T., Mayo, J.T., Yu, W.W., Kan, A.T., Colvin, V.L., and Tomson, M.B. (2005): "Effect of magnetite particle size on adsorption and desorption of arsenite and arsenate", *J. Mater. Res.*, Vol. 20, No. 12, © Materials Research Society.

Zhang, W.X. (2003): Nanoscale iron particles for environmental remediation: An overview *Journal of Nanoparticle Research* 5: 323–332.

Zhang, G., Qu, J., Liu, H., Liu, R., and Wu, R. (2007): "Preparation and evaluation of a novel Fe–Mn binary oxide adsorbent for effective arsenite removal", Water Research 41 (2007) 1921 – 1928.

বাংলাদেশ প্রকৌশল বিশ্ববিদ্যালয়
নং 107242
তাং 23.06.09
লাইব্রেরী, ঢাকা